PhD in Clinical & Experimental Medicine

UNIVERSITÀ DEGLI STUDI DEL PIEMONTE ORIENTALE

Dipartimento di Medicina Traslazionale

Corso di Dottorato di Ricerca in Medicina Clinica e Sperimentale

Ciclo XXVIII

New strategies for tissue regeneration

SSD BIO/16

Coordinatore

Prof.ssa Marisa Gariglio

Tutor

Prof. Mario Cannas

Dottorando

Dott.ssa Alessia Borrone

Table of contents

Abbreviations

ACI: Autologous Chondrocyte Implantation

ALP: Alkaline Phosphatase

ASC: Adipose Derived Stem Cells

ATP: Adenosine Triphosphate

ATX: Autotaxin

BCA: Bicinchoninic Acid

BCIP: 5-Bromo-4-Chloro-3-Indolyl Phosphate

BM-MSCs: Bone Marrow Mesenchymal Stem Cells

BSA: Bovine Serum Albumin

CAMP: Ciclic Adenosine Monophosphate

DAPI: 4', 6-diamino-2-fenilindolo cloridrato

DMEM/F12: Dulbecco's Modified Eagle Medium: Nutrient Mixture F-12

DMEM: Dulbecco's Modified Eagle Medium

DMEM-HG: Dulbecco's Modified Eagle Medium: High Glucose

DMEM-LG: Dulbecco's Modified Eagle Medium: Low Glucose

ECM: Extracellular Matrix

EGF: Epidermal Growth Factor

ERK: Extracellular Signal Regulated Kinase

FACS: Fluorescence-activated cell-sorting analysis

FAFA: Bovine Serum Albumin Fatty Acid Free

FBS: Fetal Bovine Serum

FGF: Fibroblast Growth Factors

GAG: Glycosaminoglycans

GDP: Guanosine Diphosphate

GFP: Green Fluorescence Protein

GPCR: G-Protein-Coupled Receptors

GTP: Guanosine Triphosphate

hMSC: Human Mesenchymal Stem Cell

hOB: Human Osteoblast

HSA: Human Serum Albumin

IMDM: Iscove's Modified Duolbecco's Medium

ITS: (1 mg/ml insulina, 0,55 mg/ml transferrina umana, 0,5 mg/ml selenito di sodio, 50 mg/ml albumina sierica e 470 μg/ml acido linoleico)

LIMK: LIM Kinase

LPA: Lysophosphatidic Acid

LPLs: Lysophospholipids

MACI: Matrix-induced Autologous Chondrocyte Implantation

MAPK: Mitogen Activated Protein Kinase

MLC: Myosin Light Chain

MMA: Methylmethacrylate

MSCs: Mesenchymal Stem Cells

PBS: Phosphate Buffered Saline

PI3K: Phosphatidylinositide 3-Kinase

PKC: Protein Kinase C

PRP: Platelet Rich Plasma

PS: Penicillin Streptomycin

PSF: Penicillina Streptomicina Fungizone

PTH: Paratormone

RM: Regenerative medicine

RNA: Ribonucleic Acid

ROCK: Rho-Associated Protein Kinase

SDS-PAGE: Sodium Dodecyl Sulphate - Polyacrylamide Gel Electrophoresis

SVF: Vascular Stromal Fraction

TGF-β: Transforming Growth Factor beta

TNF-α: Tumor Necrosis Factor alpha

VEGF: Vascular Endotheliar Growth Factor

WNT: Wingless-Int

1. General introduction

In the last years, tissue or organ transplantation changed reconstructive surgery field, improving the functionality of transplanted organ or tissue. These improvements were reached thanks to the understanding of the biochemical mechanisms that rule immune response of the host. Some limitations, such as the limited number of donors, the possibility of chronic rejection (that requires immunosuppressive therapies), the limited amount of suitable tissue for autotransplant and partial recovery of tissue functionality, has stimulated researcher to develop alternative strategies. Tissue engineering and regenerative medicine emerge in this context, using mostly biomaterials to repair or substitute damaged tissues. The idea of tissue regeneration is to reconstruct lost tissue or tissue function by a regenerative process. This is possible by:

1. Tissue Engineering that involve transplantation of cells in matrices.
2. Cell Transplantation that consist in injection of isolated cells.
3. Cell Homing trough an activation of resident cells.

The biomaterials used as scaffolds have to facilitate or even regulate cell processes as proliferation, migration and matrix synthesis and have to reinforce the defect (35). They should maintain the shape of the defect until the reconstruction process is finished. Additionally, the biomaterial should prevent the infiltration of surrounding tissue that may interfere with the tissue regeneration process. In some cases the biomaterials serve as a delivery vehicle for growth factors and genes that support cell processes for tissue reconstruction. It is within the framework of recent technological advances in cellular and molecular biology, engineering, materials science and especially nanotechnology that tissue engineering is

emerging to help fulfill a long-sought dream of using tissue-like materials for the replacement of tissue defects.

1. Tissue engineering can be considered basically as a three step process (36-37),(Fig. 1):

a. Cells of the desired phenotype are isolated from a small biopsy from the patient and amplified in number by means of classic cell culture techniques.

b. After the desired cell number is reached, the seeding of these cells into a scaffold is needed. The biomaterial gives the cells a temporary structure in which they further proliferate and differentiate in order to build functional organ-like units.

c. A maturation of the cell-biomaterial construct into a functional tissue mass is proceeded.

Biomaterials are grouped as synthetic (metallic, ceramic or polymeric surfaces) or natural materials, eventually biodegradable.

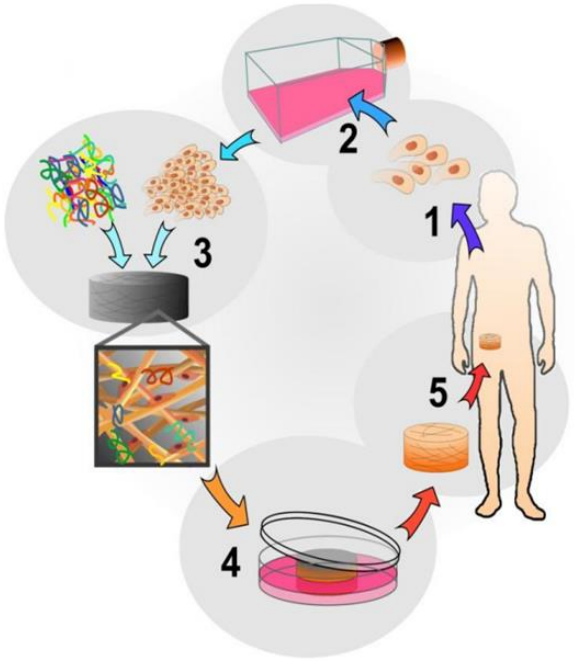

Figure 1: The tissue engineering cycle, using autologous cells. 1-A small number of cells are removed from the body. 2-Cell proliferation. 3-Cells are seeded onto porous scaffolds. 4-Theseeded scaffolds are placed in culture to further increase cell number. 5-The regenerated tissue is implanted into the site of damage. (http://www.centropede.com/UKSB2006/ePoster/images/background/TE_model_large.jpg).

2. Cell transplantation consists in the collection of cells from patients or donor, processing of the cells, and the reinjection of cells in the patient (Figure 2).

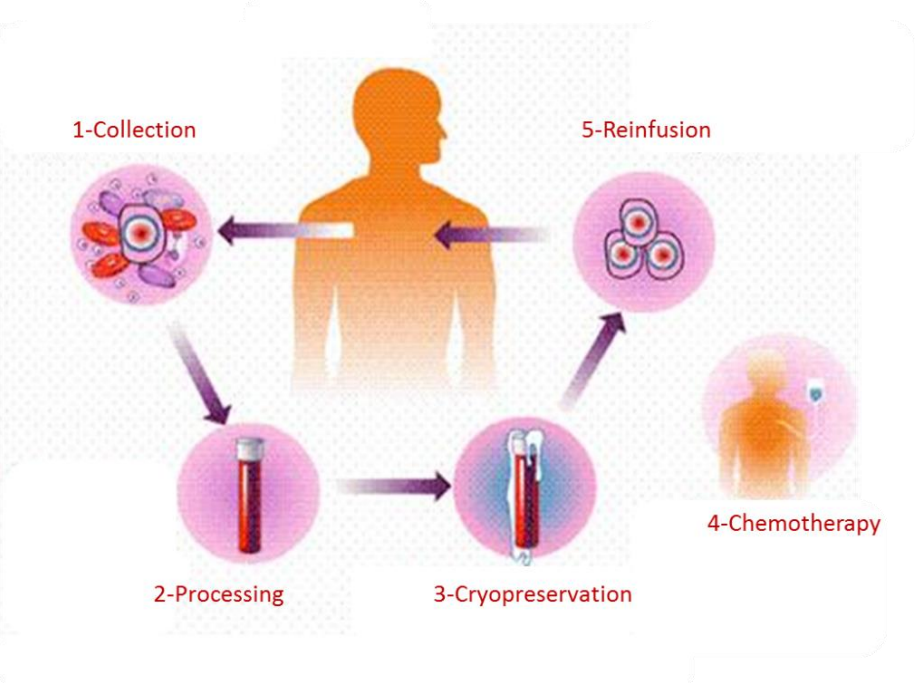

Figure 2: The autologous transplant process. 1-Collection: stem cells are collected from the patient's bone marrow or blood. 2- Processing: Blood or bone marrow is processed in the laboratory to purify and concentrate the stem cells. 3-Cryopreservation: blood or bone marrow is frozen to preserve it. 4-Chemotherapy: high dose chemotherapy and/or radiation therapy in given to the patient. 5-Reinfusion: thawed stem cells are reinfused into the patient. (http://biomed.brown.edu/Courses/BI108/BI108_2007_Groups/group03/sources.html).

The cells can be mature cells or stem cells, like mesenchymal stem cells (MSCs). Stem cell transplantation is a generic term covering several different techniques. For allogeneic transplants, hemopoietic stem cells are taken from the bone marrow, peripheral blood, umbilical cord blood or adipose tissue of a healthy donor matched for HLA type, who may be a family member or an unrelated volunteer. For autologous transplants, usually, stem cells are taken from patients'own bone marrow or adipose tissue. Interestinghy, adipose tissue is readily available in large quantities and can be obtained through less invasive procedures; it contains up to 2% of MSCs (ASC) compared with only 0.02% in bone marrow (BM-MSC). Stem cells have been used routinely for more than three decades to repair tissues and organs damaged by injury

or disease. The prospect of exploiting stem cells more widely in regenerative medicine was encouraged by the growing evidence that various adult cells retained greater versatility than had been suspected to date (38). The aim is to employ stem cells as a source of appropriately differentiated cells to replace those lost through physical, chemical or ischaemic injury, or as a result of degenerative disease.

3. The other possibility in regenerative medicine is cell homing by endogenous cells supplied from the defect area, without the necessity of cell transplantation (Figure 3).

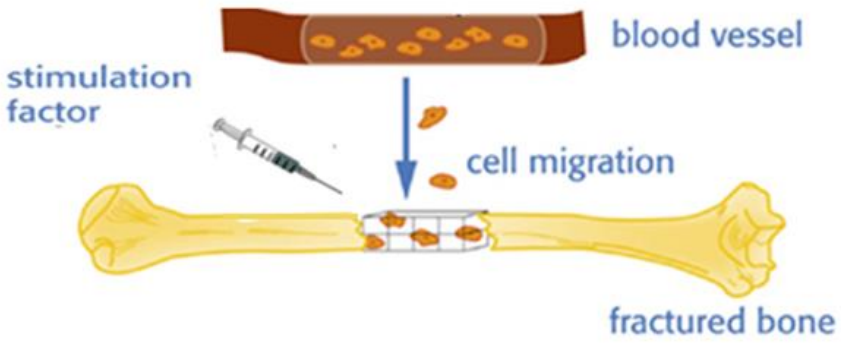

Figure 3: Homing and mobilization of native cells for bone regeneration. Homing factors are directly delivered to the defect site. Native cells may be mobilized by the administration of a stimulation factor .

Most insights (39) in the mechanisms underlying migration and homing are from studies that evaluated the migration into inflamed tissue of leukocyte (40), hematopoietic stem cells (HSCs) (41) and metastatic cancer cells (42).

A significant body of literature also exists related to the mechanism of MSCs migration towards target tissues and the role of cell surface receptors and molecules in the process. The role of activated endothelial cells in migration of MSCs is being also extensively studied. The migration of cells from the side of defect, together with an appropriate scaffold which can facilitate cell migration, could be important, for example, to speed-up bone healing and bone regeneration.

Different approaches have been used to deliver homing factors to the fracture site. In scaffold-based tissue regeneration strategies, homing factors can be covalently bound or absorbed to the scaffold. Drug delivery systems such as hydrogels, microspheres, and nanoparticles have been used on their own or in combination with scaffolds and/or biomaterials. Of note, the carrier material has a significant impact on the release profile of the homing factors.

2. Aim of the project

My PhD project is divided in two parts, focusing on the development of new strategies for orthopedic tissue regeneration. In particular, the first part is about cartilage regeneration using human lipoaspirate as autologous injectable active scaffold for one-step repair of cartilage defects, the second part is about bone regeneration, through an injectable medicated graft substitute active on bone tissue regeneration.

I. Cartilage regeneration

Research on mesenchymal stem cells from adipose tissue (ASC) shows promising results for cell-based therapy in cartilage lesions: in these studies cells have been isolated, expanded, and differentiated *in vitro*, before transplantation into the damaged cartilage, or onto materials used as scaffolds to deliver cells to the impaired area. The present study employed *in vitro* assays to investigate the potential of intra-articular injection of micro-fragmented lipoaspirate, as a one-step repair strategy; it aimed to determine whether adipose tissue can act as a scaffold for cells naturally present at their anatomical site. Cultured clusters of lipoaspirate showed a spontaneous outgrowth of cells with mesenchymal phenotype and with multi-lineage differentiation potential. Transduction of lipoaspirate clusters by lentiviral vectors expressing GFP underlined the propensity of the outgrown cells to repopulate fragments of damaged cartilage. On the basis of the results, which showed an induction of proliferation and extracellular matrix (ECM) production of human primary chondrocytes, it was hypothesized that lipoaspirate may play a paracrine role. Moreover, the structure of a floating culture of lipoaspirate, treated for three weeks with chondrogenic growth factors, changed: tissue with a high fat component was replaced by a tissue with a lower fat component and connective tissue rich in glycosaminoglycan (GAG)

and in collagen type I, increasing the mechanical strength of the tissue. From these promising *in vitro* results, it may be speculated that an injectable autologous biologically-active scaffold (lipoaspirate), employed intra-articularly, may: 1) become a fibrous tissue that provides mechanical support for the load on the damaged cartilage; 2) induce host chondrocytes to proliferate and produce ECM; 3) provide cells at the site of injury, which could regenerate or repair the damaged or missing cartilage.

II. Bone regeneration

With the aim to obtain an injectable medicated scaffold, which speeds bone formation in sinus lift augmentation, in bony void and in fracture repair, we have developed a three-dimensional (3D) jelly collagen containing Lysophosphatidic acid (LPA) and 1a,25-Dihydroxyvitamin D3 (1,25D3) using soluble native collagen prepared from rat tail tendons. We have demonstrated with an *in vitro* 3D culture model of bone fracture an osteoblasts'Rho-kinase mediated contraction of the collagen that causes an approach of human bone trabecular fragments with the formation of new union tissue within 3 weeks of organ culture. The contraction was faster in LPA medicated collagen while 1,25D3 enhanced the mineralization of the new formed tissue that showed also increased tensile strength. LPA was shown to modulate gel contraction rate not only mechanically, working in cytoskeleton reorganization, but also osteoconductively evidencing activity on proliferation, differentiation and migration of human primary osteoblasts (hOB). When LPA was used in combination with 1,25D3 a synergism on hOB's activity in term of alkaline phosphatase and mineralization was seen. On the basis of these data, collagen can be considered as an injectable natural scaffold that allows the migration of cells from the side of bone defect and its enrichment with LPA and 1,25D3 could be used *in vivo* to accelerate bone growth and fracture healing.

3. Cartilage regeneration

3.1 Introduction

The treatment of degenerative joints is becoming a very frequent necessity. Increased life expectancy and inappropriate medical treatments (e.g. removal of the meniscus) are leading to an increase of chondropathies and osteoarthritis, which also occurs at a relatively young age. Chondrocytes are the parenchymal cells of cartilage, and have limited regenerative capacity; thus after traumatic injury, the cartilage undergoes degenerative changes, which may be irreversible (18). The more superficial lesions tend to progress towards degeneration (29); those that penetrate the subchondral bone progress towards the formation of fibro-cartilage tissue. This differs from normal hyaline cartilage in both biomechanical and biochemical properties, and frequently undergoes subsequent degeneration (30). Any cartilage lesion should therefore be considered as the beginning of a chronic degenerative disease, with little chance of cure, due to the poor regenerative capacity of this type of cell (7).

Modern treatments for damaged cartilage and for the prevention of osteoarthritis include the intra-articular administration of hyaluronan (15), treatment with platelet rich plasma (PRP) (3), bone-marrow stimulation techniques (subchondral drilling, abrasion, micro-fracture) (24), osteochondral grafting (mosaicplasty) (23), autologous chondrocyte implantation (ACI), and matrix-assisted autologous chondrocyte implantation (MACI) with autologous chondrocytes cultured on collagen membranes prior to re-implantation (11). Chondrocyte-based therapy has demonstrated promising clinical results, but the procedure requires an invasive protocol, in which autologous cartilage is harvested from the patient at a healthy anatomical site. This produces damage to the normal cartilage at that site leading to pathological changes. It is

therefore evident that to avoid the disadvantages arising from the use of autologous chondrocytes, alternative cell sources must be investigated. Mesenchymal stem cells (MSCs) obtained from adult tissues of different origins (umbilical cord blood, adipose tissue, bone marrow, synovial membranes, periosteum and muscle) have recently been investigated, and their chondrogenic potential assessed and compared (28,34,14). Bone marrow and adipose tissue are the most readily available sources of MSCs. Moreover, adipose tissue is readily available in large quantities and can be obtained through less invasive procedures; of the many cell types contained in adipose tissue, MSCs (ASCs) comprise up to 2%, whereas only 0.02% of cells in bone marrow are MSCs (BM-MSCs) (20). MSCs have shown promising results for cartilage repair (31); however, in the studies published to date, cells were isolated from the originating tissue, then expanded and differentiated *in vitro*, prior to transplantation into the damaged cartilage or seeding in materials used as scaffolds to deliver cells to the injured area. No optimal stimulation regimen has yet been proposed to differentiate stem cells into chondrocytes prior to implantation; further difficulty lies in the large number of processing steps (enzymatic digestion, cell expansion and differentiation), which increases the translational barriers.

With the aim of avoiding excessive handling of stem cells and side effects derived from the scaffolds used for cell-based cartilage repair, this *in vitro* study investigated whether the intra-articular injection of autologous lipoaspirate might be an alternative cell-based therapy in treating cartilage diseases and in preventing osteoarthritis. Lipoaspirate is a natural scaffold rich in stem cells which, once injected into the intra-articular space, might give rise to different biological responses. To determine whether lipoaspirate can lead to the outgrowth of cells to the damaged cartilage, thus repopulating and repairing it, and whether lipoaspirate may have a paracrine effect on resident chondrocytes, we studied *in vitro*: 1) the ability of resident cells in

lipoaspirate to grow out from adipose tissue; 2) the phenotype of these outgrowing cells, together with their differentiation potential and their capability of repopulating an organ culture of human cartilage; 3) the effect of the lipoaspirate on the proliferation rate of human chondrocyte, and on their production of cartilaginous matrix. Furthermore, with the aim of determining whether lipoaspirate clusters might differentiate into a different tissue at the intra-articular site, thus providing intra-articular mechanical reinforcement, the chondrogenic differentiation of cells not extracted from lipoaspirate, but simply at their own natural anatomical site, was examined.

3.1.1 Cartilage tissue

Cartilage is a connettive tissue consisting of a dense matrix of collagene fibres and elastic fibres embedded in a rubbery ground substance. The matrix is produced by cells called chondroblast, which became embedded in the matrix as chondrocytes. They occur, either singly or in group , within spaces called lacunae in the matrix. The surface of most of the cartilage in the body is surrounded by a membrane of dense irregular connective tissue called perichondrium. Cartilage doesn't contain blood vessels or nerves, except in the perichondrium. There are three different type of cartilage that have slightly different structures and functions. They are hyaline cartilage, fibrocartilage and elastic cartilage (Figure4).

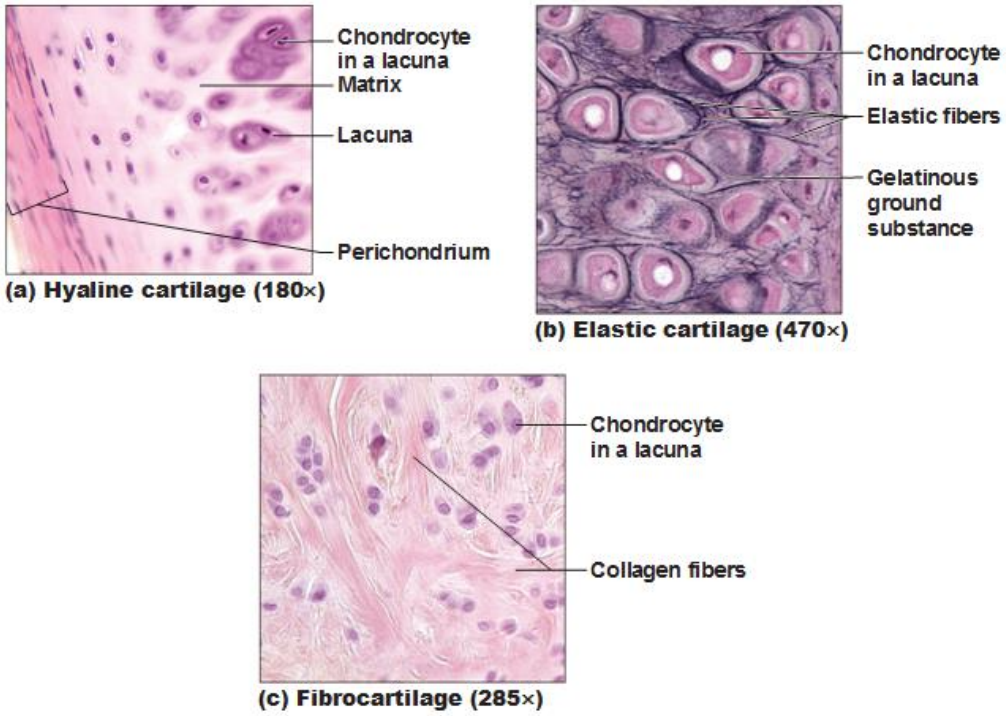

Figure 4: Types of Cartilage. (a) Hyaline cartilage provides support with some flexibility. (b) Elastic cartilage provides firm but elastic support. (c) Fibrocartilage provides some compressibility and can absorb pressure. September 27, 2011 By Antranik.

Hyaline cartilage is semi-transparent and appears bluish-white in colour. It is extremely strong, but very flexible and elastic. Hyaline cartilage consists of living cells, chondrocytes, which are situated far apart in fluid-filled spaces, the lacunae. There is an extensive amount of rubbery matrix between the cells and the matrix contains a number of collagenous fibres. Hyaline cartilage occurs in trachea, the larynx, the tip of the nose, in the connection between the ribs and the breastbone and also the ends of bone where they form joints. Temporary cartilage in mammalian embryos also consists of hyaline cartilage.

Fibrocartilage is an extremely tough tissue. The orientation of the bundles depends upon the stresses acting on the cartilage. The collagenous bundles take up a direction parallel to the cartilage. Fibrocartilage is found as discs between the vertebrae between the pubic bones in front

of the pelvic girdle and around the edges of the articular cavities such as the glenoid cavity in the shoulder joint.

Elastic cartilage is similar to hyaline cartilage, but in addition to the collagenous fibres, the matrix of the elastic also contains an abundant network of branched yellow elastic fibres. They run through the matrix in all directions. This type of cartilage is found in the lobe of the ear, the epiglottis and in parts of the larynx.

In humans, chondrocytes represent only about 1% of the volume of hyaline cartilage but are essential since are these cells that replace degraded matrix molecules, in order to maintain the correct size and mechanical properties of the tissue (43). Thus, microscopically, the cells' endoplasmic reticulum and Golgi apparatus are prominent. In addition, many contain lipid and glycogen stores and secretory vesicles. Some chondrocytes have cilia that extend from the cell into the ECM and are believed to play a role in sensing the mechanical environment of the cell, since chondrocytes are known to modify matrix properties in response to loading (44).

Chondrocytes originate from MSCs found in the bone marrow of mature individuals. During embryogenesis, the MSCs start to differentiate into chondrocytes and secrete a cartilaginous matrix. During this time, the cells continue to divide. They pass through various lineage states and eventually the chondrocytes in the central zone, located next to what will soon be bone, enter the final stage of development and become hypertrophic chondrocytes, producing proteins that are important in the calcification of the matrix. Other chondrocytes (on the periphery) secrete collagen and matrix molecules in the right proportions to produce hyaline cartilage. Mature articular chondrocytes, unable to proliferate, appear rounded and are completely encased in matrix (44,45).

3.1.2 Articular cartilage injury

Articular cartilage has very limited capability to heal. Cartilage disruption results in progressive loss of joint motion, pain and disability, decreasing the quality of life of the affected person (46). Globally, the number and severity of cases are on ascending trend, increasing the burden of disease and taking a high toll on healthcare resources (47). Articular cartilage covers bone surfaces within a joint, functioning as a shock absorber and facilitates motion. Its structure is adapted to functioning under high compression, tensile and shear stress. This ultra specialized tissue is aneural, avascular and alymphatic with low cellularity, high extracellular matrix content and a stratified cell-fiber distribution. The nourishment of a relatively low cell population is provided by nutrient diffusion from subchondral bone vessels and synovial fluid. The same structural particularities, which are the basis of the remarkable biomechanical endurance, are considered to be the principal cause of the incapacity to heal after trauma and degeneration (48). There are three main types of cartilage injury: matrix disruption, partial thickness defects, and full thickness defects. Matrix disruption occurs from blunt trauma, such as dashboard injuries in automobile accidents. The ECM is damaged, but if the injury is not extreme, the remaining viable chondrocytes will increase their synthetic activity to repair the tissue. Partial thickness defects demonstrate disruption of the cartilage surface (fissures, etc.) but this does not extend to the subchondral bone. Immediately following the injury, nearby cells begin to proliferate, but for reasons that remain unclear, cellular attempts to fill the defect cease before it is repaired. Full thickness defects arise from damage that transverses the entire cartilage thickness and penetrates the subchondral bone. In this case, the defect is filled with a fibrin clot and a classic wound healing response ensues. With this type of injury, unlike the others, there is access to a population of progenitor cells from the bone marrow which can migrate to fill the defect (49,

50). These cells usually cause replacement of the fibrin clot with tissue intermediate between hyaline and fibrocartilage. This tissue is usually less stiff and more permeable than native cartilage, which could contribute to its eventual degradation over a period of months (50).

Several factors may explain why cartilage demonstrates very little capability for self-repair after injury. Chondrocytes are not required to proliferate to maintain cartilage, as in other tissues (i.e. skin), and mature chondrocytes have a relatively low metabolic activity (44). Except in the case of full-thickness defects, there is no direct access to progenitor cells (such as are found in bone marrow) and the resident chondrocytes may be impeded by the ECM from migrating to fill the defect (49,51). In addition, the proteoglycans in the ECM can prevent cell adhesion, further undermining the native repair process (51).

3.1.3 Cartilage repair and regeneration

The attempt to cure the cartilage injury remains still frustrating to modern orthopedic surgery (52). Different methods of grafting make use of autologous or allogeneic cartilaginous or non-cartilaginous tissues to fill joint surface defects (53). Procedures that stimulates subchondral bone, such as subchondral drilling, microfracture, and abrasion arthroplasty are used to create controlled microlesions within the osseous tissue underlying the defect. The blood clot produced by such procedures is rich in bone marrow progenitors and is thought to induce cartilage repair (54). These interventions are capable to generate short term satisfactory results reducing pain and restoring mobility. Their major drawback is the poor quality of the repair tissue. The fibrous cartilage does not reproduce the structural organization and the mechanical endurance of the native hyaline joint surface. Such repair is prone to progressive clinical and morphological deterioration followed by the generalized joint failure (55). Regenerative medicine (RM) is

introducing the concept of complete structural and functional restoration of tissues, organs and systems made possible by the use of breakthrough discoveries in the field of molecular cell and developmental biology (56). It is sought that using RM specific tools, complete structural regeneration and functional rehabilitation of affected joint would be possible. Biological joint restoration and complete re growth of hyaline cartilage could address both traumatic defects as well as tissue deterioration. To this end, a wealth of basic and translational research is currently going on. Specific RM strategies, cell therapy, tissue engineering or gene therapy are in different stages of preclinical testing or clinical applicability. Introduced in the early 1990's by a Swedish group, autologus chondrocyte implantation (ACI) uses a cell suspension of autologus adult cells to treat focal cartilage defects (57). A development of ACI, the matrix assisted chondrocyte implantation/transplantation (MACI/MACT), can be considered a form of cartilage engineering (Figure 5).

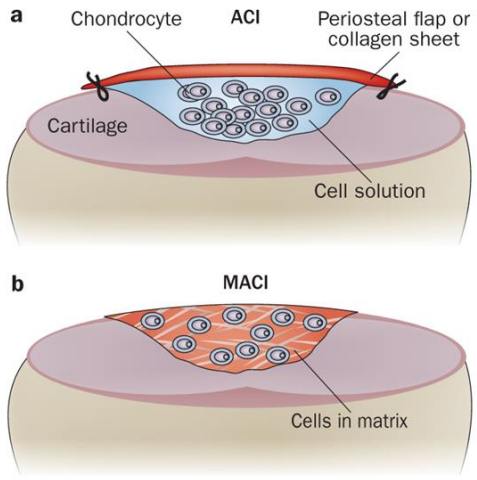

Figure 5: Major principles for the regenerative treatment of cartilage lesions. a) During ACI, chondrocytes are harvested from a small cartilage biopsy sample, cultured and implanted as a cell suspension into a cartilage defect. To prevent a leakage of cells, the defect is covered by a periosteal flap or collagen sheet. b) During MACI, isolated and culture-expanded chondrocytes are seeded into matrices. Besides other advantages, such as homogeneous cell distribution, initial mechanical stability and simplified surgical handling, over ACI, such grafts can be fixed onto subchondral bone, which, therefore, enables a stable fixation in diffuse defects. (Nature Reviews Rheumatology 8, 493-498 (August 2012)).

With this procedure, cells are delivered to the cartilage defect by means of a three-dimensional matrix thereby improving their retention and enhancing their biological activity at implantation site (58). Currently several scaffolds and methods of cell seeding are commercially available (59, 60). However, the clinical advancement of adult cell based therapy is limited by technical inconveniences, cell source related obstacles as well as by the availability and affordability of the procedure. Having an increased proliferative and differentiation potential, MSCs are looked upon as a suitable cell source for cartilage regeneration. Case series of succesful use of MSC to treat cartilage defects are reported (61). Several clinical trials using autologus or allogeneic MSCs for cartilage regeneration are going on (62).

3.1.4 Stem cells

Stem cells have been used routinely for more than three decades to repair tissues and organs damaged by injury or disease. The prospect of exploiting stem cells more widely in regenerative medicine was encouraged by the growing evidence that various adult cells retained greater versatility than had been suspected hitherto (38). The aim is to employ stem cells as a source of appropriately differentiated cells to replace those lost through physical, chemical or ischaemic injury, or as a result of degenerative disease.

The ideal stem cell for use in functional tissue engineering needs to be abundantly available, harvested with minimal morbidity, differentiated reliably down various pathways and able to be transplanted safely and efficaciously. Stem cells exist in an undifferentiated state, and exhibit both the capacity to self-renew, and the capability to differentiate into more than one type of cell (73). Although embryonic stem cells seem to exhibit unlimited differentiation potential both *in vitro* and *in vivo*, they are subject to significant ethical, legal and political concerns and are

not generally available in current medical practice or research. Stem cells from adult tissue, on the other hand, suffer from few such restrictions. Multipotent stem cells can be isolated from various mesenchymal tissue sources in adults, most commonly bone marrow. The harvest of BMSC has practical constraints. These include pain at the harvest site, and harvest of only a small volume of bone marrow (and therefore a small number of stem cells), meaning that they are likely to require *ex vivo* expansion of the cells to obtain clinically significant cell numbers. Umbilical cord blood (UCB) from the placenta of term infants also contains mesenchymal stem cells. The use of UCB has been limited by the practical difficulties in obtaining and isolating the mesenchymal stem cells at the time of birth and ensuring adequate long-term storage for autologous use, and the fact that their differentiation potential seems to be lower than that of BMSC (63). Adipose tissue is derived from embryonic mesoderm. As MSCs, the isolated cells are capable of forming bone, cartilage and muscle, as well as fat (64-68) (Figure 6). These stem cells have been variously termed pre-adipocytes, stromal cells, processed lipoaspirate cells, multipotent adipose-derived stem cells, and adipose-derived adult stem cells. A recent consensus reached by investigators at the 2004 conference of the International Fat Applied Technology Society has settled on the term ‘adipose-derived stem cells’ (ASC) (69). Abundant numbers of ASC can be derived from lipoaspirate, the waste product of liposuction surgery. The yield compares favourably with a bone marrow aspirate (70). Compared with BMSC, ASC are more easily cultured and grow more rapidly (71, 72). They can also be cultured for longer than BMSC before becoming senescent (63). All of these qualities make ASC a useful source of mesenchymal stem cells.

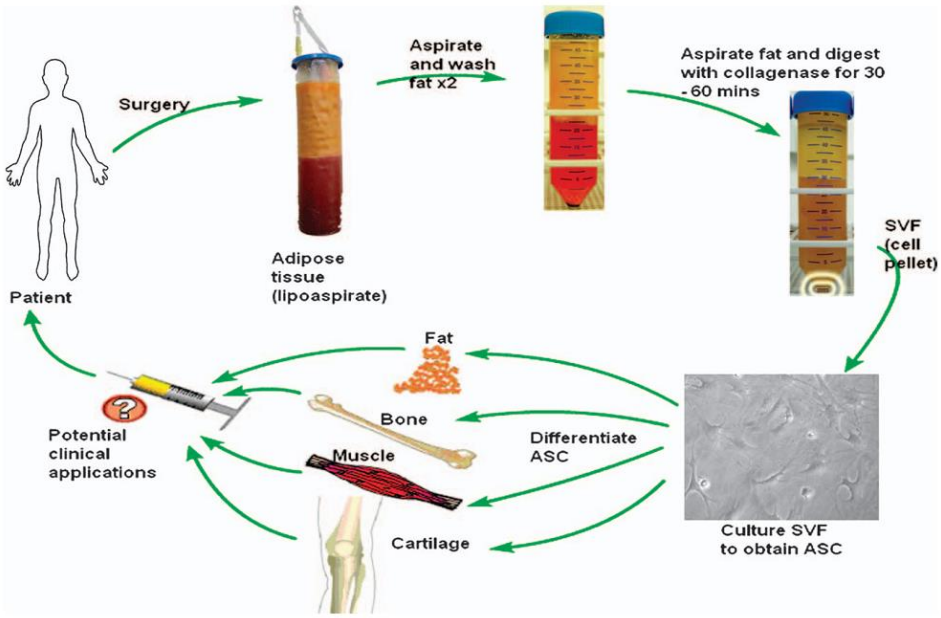

Figure 5: Summary of cycle of human adipose-derived stem cell (ASC) isolation and differentiation for clinical usage. SVF, stromal vascular cell fraction.

3.2 Materials and Methods

3.2.1 Materials

Lipoaspirates were obtained from five healthy female patients (age range 30-45) undergoing an elective liposuction from a single anatomical site (abdominal subcutaneous fat tissue) at the IMAGE Institute (Milan, Italy). The ethical committee of the University of Milan approved the design of the study. Exclusion criteria were: body mass index (BMI) >30, diabetes, hypertension, and nicotine or alcoholic abuse. Written informed consent, specifying that residual material destined to be disposed of could be used for research, was signed by each participant before the biological materials were removed, in agreement with Rec(2006)4 of the Committee of Ministers Council of Europe on research on biological materials of human origin. After a preliminary infiltration of 400ml of saline solution, with adrenaline 2µg/ml (S.A.L.F. Spa., Bergamo, Italy) as a vasoconstrictor and lidocaine 0.02% (AstraZeneca, Luton, UK) as an

anesthetic, the aspiration was performed using a 10cc syringe with a Luer-Lok® tip (BD Medical, VWR Int., Milano, Italy) connected to a disposable 19 cm blunt cannula (3mm OD), with 5 oval holes (1x2mm). From each of five patients, 210 ml of lipoaspirate were obtained and processed as follows, giving four batches of lipoaspirate. 10 ml were washed with 25 ml phosphate buffered saline (PBS) (Sigma-Aldrich, Milan, Italy) on a 250 μm Nitex filter (Dutscher Scientific, Essex, UK) and used as control (CTR); 50 ml were centrifuged for 3 minutes at 1500 x g (22) and 10 ml used as Coleman (Col); 50 ml were processed with a commercial device (PureGraft® Cytori Therapeutics, San Diego, CA, USA) according to the manufacturer's instructions (25) and 10 ml used (PurGr); 100 ml were processed with a commercial device (Lipogems®, Lipogems Int. S.p.A., Milano, Italy) that washes and micronized lipoaspirate (4) following the manufacturer's instructions and 10 ml used (LipoG).

3.2.2 Chondrogenic organ culture model

500 μl of each batch of lipoaspirate were cultured as free-floating aggregates, in a conical polypropylene centrifuge tube (EuroClone, Milan, Italy) in 4 ml of chondrogenic medium containing 1 ml Dulbecco's Modified Eagle Medium (DMEM–high glucose Sigma-Aldrich), ascorbate-2-phosphate (100 μM, Sigma), dexamethasone (10^{-7} M, Sigma) and 1% Insulin-Transferrin_Selenite (ITS+1 media supplement, Sigma) for 3 weeks at 37°C in a humidified atmosphere containing 95% air and 5% CO_2. The tubes were gently shaken daily, to allow the culture media to cover the sample, which otherwise tended to float. Half of the culture medium was changed twice a week with the addition of fibroblast growth factor 2 (FGF2) and transforming growth factor beta 2 (TGFβ2) found in previous research to be chondrogenic on bone marrow stem cells (6). Replicate aggregates from each batch of lipoaspirate were

processed for the following determinations: histological and immunohistological evaluation, mechanical evaluations, biochemical studies, RNA extraction, and RT–PCR analysis. Before processing, digital images were taken of each lipoaspirate organ culture using a digital camera, on samples treated or not for three weeks with the chGF.

3.2.3 Mechanical evaluations

The compression properties of untreated and chGF-treated lipoaspirates were tested using an Electro Force BioDynamic Test Instrument (Bose, TA Instruments, Eden Prairie, MN, USA). Samples of 2 ± 0.5 mm^3 were positioned inside the instrument's bioreactor chamber between two pistons. Tests were performed with a constant crosshead speed of 0.05 mm/sec. The instrument showed the real-time displacement of the piston, and the force acting on the sample, producing a force/displacement curve. Compressive strength and Young modulus were then calculated, using the surface area of the sample, initial length of the sample, compressed length, and force at breaking point. All samples were tested in triplicate, and data are presented as mean ± standard deviation (SD).

3.2.4 Histology and immunohistochemistry

After 21 days of culture, neo-formed tissues were rinsed in PBS and fixed overnight in 10% buffered formalin (Diapath S.r.l., Martinengo, Italy) at 4°C. The fixed tissues were dehydrated by treatment with alcohol, embedded in paraffin, and sectioned to a thickness of 7 μm. For histological evaluation, sections were deparaffinized using xylene, rehydrated, and stained with Hematoxylin/Eosin (H&E Sigma-Aldrich) or Toluidine Blue (Sigma-Aldrich) to detect proteoglycan, or with Sirius Red F3BA (Chroma, Stuttgart, Germany) to detect collagen.

Alternate sections were used for immunohistochemistry to detect vessels: rehydrated sections were treated with 0.5% H2O2 (Sigma-Aldrich) to inactivate endogenous peroxidases, incubated in 1 mg/ml pepsin (Sigma-Aldrich) in 0.5 M acetic acid (Sigma-Aldrich) for 2 h at 37°C, blocked with 1.5% goat serum (Vector Laboratories, Burlingame, CA, USA) in PBS for 1 h at room temperature and incubated for 1 h at room temperature with anti Von Willebrand factor 25 μg/ml (DAKO, Glostrup, Denmark) and FITC-conjugated secondary antibody 10 μg/ml (Vector Laboratories).

3.2.5 Glycosaminoglycan and collagen quantification

2 mg of weighed tissue were taken after 21 days of culture, washed with PBS, and digested with 200 μl papain (1 μg/ml in 50 mM NaH2PO4, pH 6.5, containing 2 mM *N*-acetyl cysteine and 2 mM EDTA, all from Sigma-Aldrich) for 16 h at 65°C. Glycosaminoglycan were quantified by reaction with 1.9-dimethylmethylene blue (16 μg/ml DMMB, Sigma-Aldrich) (12) using chondroitin sulphate (Sigma-Aldrich) as a standard. Measurements were made with a microplate reader (BS 1000 Spectracount, Packard BioScience Company, Meriden CT, USA) at a wavelength of 530 nm. The results are reported as mean ± SD (n = 3) μg sGAG content/mg of the tissue and as % increase versus untreated sample (21 days' culture in basal medium).

Collagen was quantified according to Tullberg-Renert & Jundt (32). Briefly, 2 mg of tissue were extracted overnight at 4°C in 0.5 ml of acetic acid 0.2%, air dried and stained with 1 ml Sirius Red dye (Sigma-Aldrich) reagent (1mg/ml in saturated aqueous picric acid, Sigma-Aldrich) for 1 h. The dye solution was then removed, and the tissue was washed with 0.01 N hydrochloric acid (Sigma-Aldrich) to remove all non-bound dye; the stained material was dissolved in 0.2–0.3 ml 0.1 N sodium hydroxide for 30 min at room temperature. The optical density (OD) was

measured with a BioRad microplate reader 3550 (BioRad, Milan, Italy) at 550 nm against 0.1 N sodium hydroxide as blank. The results are reported as means ± SD (n=3) μg collagen/ml and as % increase versus the untreated sample (21 days of culture in basal medium).

3.2.6 Real-time PCR

Total cellular RNA was extracted using a Quiagen QIAsshredder kit (Qiagen, Dusseldorf, Germany) and quantified using a RiboGreen RNA quantification assay (Molecular Probes, Invitrogen, Milan, Italy). 200 ng were reverse transcribed (RT) using a High-Capacity cDNA Archive Kit (Applied Biosystems, Foster City, CA, USA). The RT thermal profile was 25°C for 10 min, 37°C for 120 min, 85°C for 5 min and kept at 4°C. Primers and probe were provided by TaqMan gene expression assay kit (Applied Biosystems) and were added to the reaction mixture according to the manufacturer's directions: SOX-9 (Hs01001343_g1), COL2A1 (Hs00264051_m1), COL1A1 (Hs00164004_m1), GADPH (Hs02758991_g1). Amplification reactions were performed with SSOFast Probes Supermix with ROX (BioRad, Milan, Italy). mRNA levels were measured by real-time RT-PCR based on TaqMan methodology, using CFX96 Real-Time System C 1000 Thermal Cycler (Bio Rad, Milan, Italy). Real-time data analysis was run with BioRad CFX Manager 2.1 software. Target gene expression was normalized to GADPH mRNA expression. Relative differential gene expression was calculated (27).

3.2.7 Isolation and culture of human Chondrocytes (hChs)

Normal human articular cartilage was obtained from the femoral or radial heads of three male subjects with displaced fractures. The mean age of the group was 33 years (range: 20–41).

Written consent was signed by each participant before biological materials were removed according to Rec(2006)4 of the Committee of Ministers Council of Europe and used after local ethics committee approval. Immediately after surgery performed at the Traumatology division of the Major Hospital of Novara, healthy cartilage was taken under sterile conditions, washed with PBS supplemented with 50 U/ml Penicillin, Streptomycin 50 μg/ml and 250 ng/ml Fungizone (PSF, all reagents from Sigma-Aldrich) and cut into pieces of approximately 2 x 2 mm, before enzymatic digestion, as follows and according to Archer et al (1): pieces were placed for 30 min at 37°C, 5% CO^2 in DMEM/F12 (EuroClone) containing Trypsin (0.25% w/v, Sigma-Aldrich) and PSF (100-120 rpm shaking); the supernatant was discarded and the cartilage fragments were further digested in DMEM/F12 with PSF containing 0.8 mg/ml collagenase II (Sigma-Aldrich) for 4 hours at 37°C, 5% CO2 (100-120 rpm shaking). The digested tissue was then allowed to settle and the supernatant containing cells was centrifuged at 1500g for 5 minutes. The cell pellet was washed with PBS-PSF and re-suspended in growth medium: DMEM/F12 supplemented with PSF, glutamine 200mM (EuroClone), ascorbic acid 50μg/ml (Sigma-Aldrich), FBS 2% (EuroClone), TGFβ 1ng/ml (Sigma-Aldrich), FGF2 1ng/ml (Sigma-Aldrich), IST^+ 10μg/ml (Sigma-Aldrich), seeded in monolayer in culture plates at low density (4000 cell/cm^2) and incubated in a CO^2 incubator at 5% CO^2, 37°C.

3.2.8 Effect of lipoaspirate on hCh proliferation and matrix production

Chondrocytes were used for the experiments within the third expansion treatment. They were plated at a density of 10^3 cells/well in a 96-multiwell plate and hChs were cultured in basal culture medium (DMEM/F12 supplemented with antibiotics, glutamine ascorbic acid, FBS 2%, TGFβ 1ng/ml, FGF2 1ng/ml IST^+ 10μg/ml as described for hChs culture and abbreviated CTR)

were compared to cells cultured in lipoconditioned culture medium made up of basal culture medium supplemented with 15% of lipoaspirate culture medium that was obtained as follows: 1 ml of lipoaspirate corresponding to 850±20 mg of tissue, was cultured in 10 ml of basal medium in a CO^2 incubator at 5% CO^2, 37°C for 4 days; upon this treatment, extracellular proteins were released into the medium. Chondrocytes were cultured in basal or in lipoconditioned culture medium for 1, 3, 6 and 12 days; after each incubation time cell proliferation and cartilaginous matrix production were assayed.

For the proliferation assay, an ATP quantification Kit (ViaLight, Cambrex Profarmaco, Milan, Italy) was used following the manufacturer's protocol; briefly, cells were lysed with cell lysis reagent, supplied with the kit, and treated with ATP monitoring reagent, which utilizes luciferase and was supplied with the kit. The light produced was measured by a luminometer (PerkinElmer) and expressed as relative luminescence units (RLUs) (9). For the cartilaginous matrix production assay 0.1 ml of each standard or culture medium to be tested were added to 0.1 ml DMMB dye in a 96 microplate wells; they were read in a micoplate reader at A525.

3.2.9 Cell outgrowth from lipoaspirate

The outgrowth of cells from Col and LipoG clusters was studied by quantifying, on the bottom of the well, the number of cells that had grown out from 50 mg of tissue/well, when the lipoaspirate was cultured in floating conditions in a 24 multiwell dish, from time 0 to 18 days. The outgrowth study was done also in a 3D matrix, as follows: to 50 µl of collagen solution, obtained from rat tail tendon (10), a cluster of lipoaspirate was added, prior to gel formation, which was achieved within 1 hour of incubation at 37°C in culture medium (DMEM with 10% FBS, 100 U/ml penicillin, 100 µg/ml streptomycin and 2 mM L-glutamine all from Sigma-

Aldrich). The kinetics of cell outgrowth, and the number of cells/mg tissue, were evaluated by quantifying 4',6-diamidino-2-phenylindole (DAPI, Sigma-Aldrich)-positive cells. Briefly, 3D collagen gels were fixed in formalin 4% for 1 hour at room temperature, and stained for 10 minutes with DAPI 300nM (Molecular Probes), before counting nuclear positivity by fluorescence microscopy (Leica Microsystems, Milan, Italy).

3.2.10 Cell phenotype characterization with flow cytometry analysis

To determine whether the mechanical and enzymatic treatments, normally used to isolate stem cells from adipose tissue for regenerative medicine applications, may be avoided, the phenotype of cells obtained by outgrowth from the clusters was compared to that of cells obtained as follows. After digestion of lipoaspirate with type I collagenase 1mg/ml in PBS (Sigma-Aldrich) at 37°C for 30-60 min, the stromal-vascular fraction (SVF) containing ASCs was obtained through centrifugation for 10 min at 450 x g. Cell pellets were re-suspended in red blood cell lysis buffer (2.06 g/L Tris base pH 7.2, Sigma-Aldrich and 7.49 g/L NH_4Cl Sigma-Aldrich) and incubated at RT for 10 min, to remove any remaining erythrocytes. Pellets were collected and filtered sequentially through 100- and 40-μm cell strainers (VWR Int., Milano, Italy) to remove undigested tissue. The pellets were then washed and the cells re-suspended in DMEM-Ham's F-12 medium (vol/vol 1:1) supplemented with 10% FBS, 100 U/ml penicillin, 100 μg/ml streptomycin and 2 mM L-glutamine, and plated in a 75 cm^2 tissue culture flask coated with collagen (Thermo Scientific, Waltham, MA, USA). ASCs were self-selected out of the SVF, based on their adherent phenotype, during subsequent tissue culture passages, after which they were maintained in a humidified atmosphere with 5% CO_2 in an incubator at 37°C. Cells were incubated with 1 $\mu g/10^6$ cells of fluorescent antibodies for 40 min at 4°C in the dark. The

antibodies used were: anti-CD146 (10µg/ml), anti-CD105 (10µg/ml), anti-CD90 (10µg/ml), anti-CD73 (5µg/ml), anti-CD45 (5µg/ml), anti-CD44 (3.5µg/ml), anti-CD34 (7.5µg/ml), and anti-CD31 (2.5µg/ml) (all from BioLegend, San Diego, CA, USA). After washing, cells were analyzed on a flow cytometer (FACSAria, BD Biosciences, San Jose, CA, USA) by collecting 10,000 events, and the data were analyzed using the FACSDiva Software (BD Biosciences).

3.2.11 Cell differentiation capacity

To confirm the mesenchymal activity of those cells that grew out naturally from the lipoaspirate clusters, while under culture conditions, their *in vitro* differentiation capacity was studied according to Noel et al (26). Briefly, 10 x 10^3 cells/cm2 were cultured in DMEM-low glucose supplemented with 10% FBS, 0.5 mM isobutyl-methyl xanthine (IBMX, Sigma-Aldrich), 200 µM indomethacin, 1 µM dexamethasone, and 10 µg/ml insulin (all from Sigma-Aldrich); after 2 weeks they were stained with fresh oil red-O solution (Sigma-Aldrich) for adipogenesis; after 3 weeks of culture in DMEM-low glucose supplemented with 10% FBS, 10 mM β-glycerophosphate, 0.2 mM ascorbic acid, and 10 nM dexamethasone (all from Sigma-Aldrich), for osteogenic differentiation, cells were stained with Calcein solution (Sigma-Aldrich) to evidence mineralization (16) and with 5-Bromo-4-chloro-3-Indolyl phosphate (BCIP, Sigma-Aldrich) to evidence alkaline phosphatase activity (8). To demonstrate chondrogenic differentiation, pellets of 5 x 10^5 cells were cultured for 3 weeks in chondrogenic medium (Lonza, Cologne, Germany), formalin-fixed, embedded in paraffin, and immunostained for Type II collagen by incubation with rabbit polyclonal anti-collagen type II primary antibody 1 µg/ml (Biogenesis, Oxford, UK) and with secondary antibody conjugated to peroxidase (Vector Laboratories).

3.2.12 Transduction and Examination of Lenti-GFP lipoaspirates

High-titer VSV-pseudotyped lentiviral vectors (LV) were produced in human embryonic kidney 293T cells (ATCC® CRL-3216™) by transient transfection with the lentiviral transfer vector construct pCCLsimPPT.PGK.GFP.WPRE (Lenti-GFP) and purified by ultra-centrifugation, as described by Follenzi et al (13). Expression titers for green fluorescent protein (GFP)-expressing vectors were determined on 293T cells by fluorescence-activated cell-sorting (FACS) analysis (FACSCalibur; BD Biosciences Immunocytometry Systems, San Jose, CA, USA) and was between 5×10^9 and 10^{10} transducing units (TU)/ml. Clusters of lipoaspirate were transduced by Lenti-GFP into serum-free DMEM for 24 hours at 37°C at several concentrations of LV particles (10^8-10^6 TU/ml), and the most efficient concentration was selected after 48 hours by scoring GFP-positive cells using fluorescence microscopy. The transduction efficiency was determined by counting GFP-positive and -negative cells in at least 10 representative high-power fields against DAPI (DAPI; D-1306; Molecular Probes).

3.2.13 Evaluation of the repair of damaged cartilage

GFP-LipoG clusters were co-cultured with an organ culture of healthy or mechanically damaged cartilage, obtained from head of the femur of one of the three fracture cases, and cultured in a 24-well plate in DMEM/F12 supplemented with PSF, glutamine (200mM), ascorbic acid (50μg/ml), FBS 2%, TGFβ (1ng/ml), FGF2 (1ng/ml), and IST^+ (10μg/ml). At 1, 3, 6, 12 and 24 days after the beginning of the culture, fluorescence microscopy was used to detect whether GFP-positive cells had migrated out from the lipoaspirate, to populate the cultured cartilage. To determine whether cells originating from the lipoaspirate (GFP positive cells) that had repopulated the damaged cartilage, had differentiated into chondrocytes, SOX-9-Texas Red

(Santa Cruz Biotechnology, Heidelberg, Germany) immunostaining was applied. The repopulated cartilage was formalin fixed and after 1 h incubation in 5% goat serum and 0.2% Triton X-100 (Sigma-Aldrich) in PBS it was incubated 1 h at room temperature with a rabbit polyclonal antibody for SOX-9 2µg/ml (Santa Cruz Biotechnology, Heidelberg, Germany) and a Texas Red conjugated secondary antibody 10µg/ml (Vector Laboratories).

3.2.14 Statistical analysis

The data were analyzed statistically using the SPSS for Windows software package (Statistical Package for Social Science, IBM, Armonk, NY, USA). Multiple comparisons of data were performed using one-way analysis of variance (ANOVA) and Bonferroni post hoc tests were applied to evaluate differences in mechanical properties, biochemical results, real-time PCR, and FACS. The p value was obtained from the ANOVA table; the conventional $p \leq 0.05$ level was considered to reflect statistical significance.

3.3 Results and Discussion

3.3.1 Chondrogenicity of lipoaspirate

Morphological, mechanical, biochemical and molecular characterization showed that treatment of the lipoaspirate organ culture with the combined chondrogenic growth factors, induced the formation of a tissue completely different from the starting material and from that treated for 3 weeks in basal medium. Comparing the four lipoaspirates obtained with the four techniques described above, the washed lipoaspirate and that obtained with Col technology showed similar behavior, while that obtained with the LipoG technique produced the most significant changes in cellular organization, in mechanical properties of the new-formed tissue, and also in its microscopic and molecular aspects. From the macroscopic image (Fig. 6 A and B) it can be seen that the structure of all lipoaspirates changed after 3 weeks of treatment with chondrogenic factors; the compactness of the tissue had increased in all cases. However, the Col and PurGr lipoaspirates started from a tissue with a more compact texture than that of the LipoG batch; before treatment, the latter was characterized by individual isolated micronized fat globules of 0.4 ± 0.1 mm^2 whereas Lipoaspirate, Col and PurGr batches contained clusters of 1.8 ± 0.9 mm^2. The new-formed tissues also showed statistically-relevant differences in mechanical properties, measured under compression, using a Bose Electoforce instrument. The aggregation of the starting tissue was particularly evident in the case of the LipoG which generated a compact structure, with about 270% increase compared to the starting value in both tensile strength (Fig. 6C) and Young modulus (Fig. 6D). In Figures 6C and 6D are indicated with A samples before the 3 weeks of culture in the chondrogenic model and with B samples after the 3 weeks of culture in the chondrogenic model.

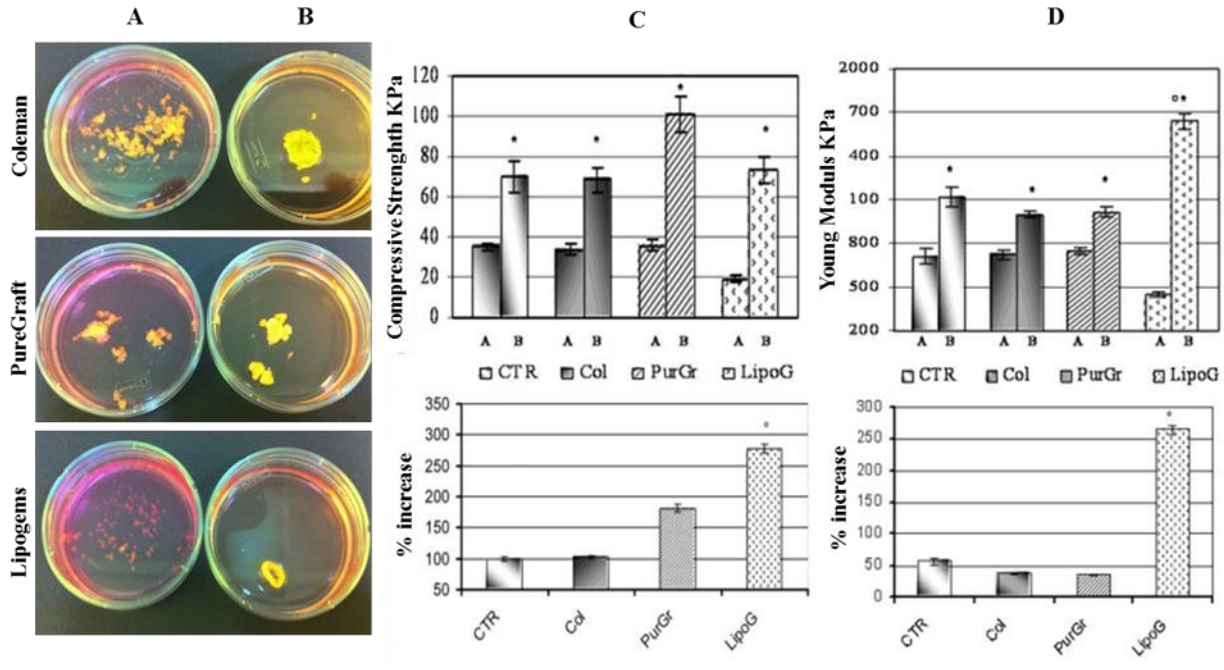

Figure 6: Macroscopic results (A before; B after 3 weeks' culture with chondrogenic factors). C and D show mechanical results, respectively as Compressive Strength and Young Modulus. The upper bar graph shows the results of samples before treatment (A) and after 3 weeks' culture in the chondrogenic model (B); the lower graph shows the % increase following treatment. Results are expressed as mean ± SD of two experiments for each patient (n=10). *p<0.05 sample B compared to sample A. °p<0.05 compared to the other samples.

The histological and immunohistological analysis also showed considerable tissue modification (Fig. 7) with a reduction of the fatty component in favor of a connective tissue rich in GAGs (Fig. 7B), in collagen (Fig. 7C), and with a reduced presence of blood vessels (Fig. 7D). Comparing the histology of the lipoaspirates obtained with the four techniques tested the LipoG batch (Panel 4, Fig. 7) underwent the most significant changes in cellular organization, with only a few areas of adipose tissue, the remainder being almost completely replaced by collagen and GAGs. These data were confirmed by the biochemical quantifications, shown in Figure 8A for GAG and Figure 8B for collagen. Since the PurGr batch of lipoaspirate gave the poorest performance in the preliminary experiments for the remainder of the study only the CTR, Col and LipoG batches were employed. Real-time PCR showed that, before treatment, all three

lipoaspirates expressed similarly low levels of collagen type I, whereas none expressed mRNA for collagen type II, nor for Sox9, at 40 cycles of PCR reaction. After three weeks' treatment in chondrogenic culture medium, the mRNA of lipoaspirate clusters was altered in a similar direction, with an increase of gene expression of collagen type I, and a small increase of gene expression of Sox9 (Fig. 8C). The increase in Sox9 gene expression was particularly evident in the LipoG batch. No collagen type II was detected.

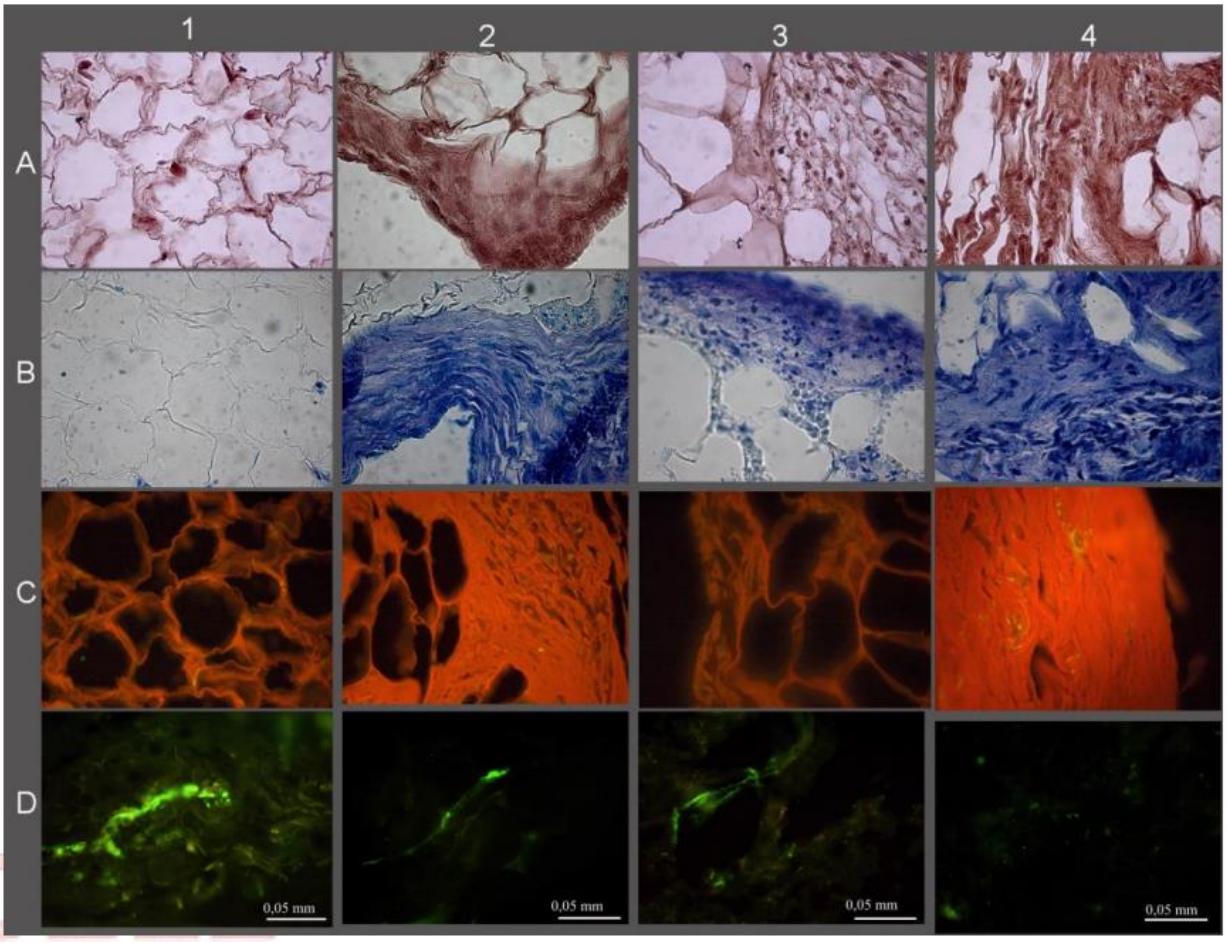

Figure 7: Histological and histochemical results; A-Hematoxylin/Eosin; B-Toluidine Blue; C-Sirius Red; D-VonWillebrand. 1- CTR lipoaspirate before chondrogenic treatment; 2, 3, and 4- respectively Col, PurGr, and LipoG batches after 3 weeks' treatment with chondrogenic factors.

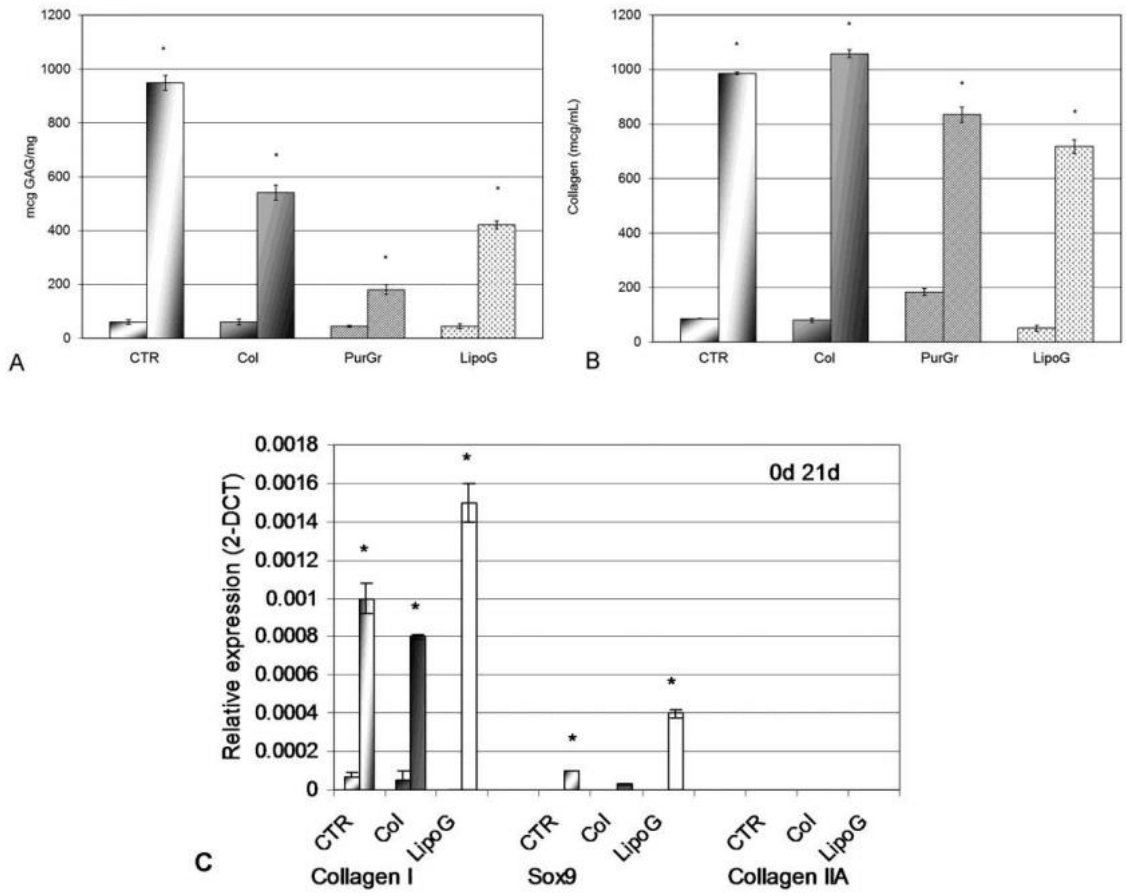

Figure 8: Biochemical quantification of GAG expressed as mg GAG per mg tissue (Figure 8A) and of total collagen expressed as absolute value in µg/mL (Figure 8B). Expression of chondrocytic markers in lipoaspirate tissue extracts normalized with GAPDH and reported as relative differential gene expression (Figure 8C). For each sample, the reported values are from samples before (first column) and after (second column) chondrogenic treatment (21 days' culture in chGF enriched chondrogenic medium) *$p<0.05$ compared to the sample before chondrogenic treatment. The results are given as means ± SD (n = 3).

3.3.2 Effect of lipoaspirate on chondrocytes

Culture medium from both Col and LipoG lipoaspirates was found to induce chondrocyte proliferation and ECM production to the same extent. As shown in Fig. 9A, already 3 days after the addition of 15% lipoaspirate culture medium, a statistically-significant increase in ATP levels occurred in both cases compared to the CTR. This increase was more evident at longer incubation times, reaching a plateau at 18 days of culture, with 80% more ATP in chondrocytes treated with 15% culture medium of the lipoaspirate and LipoG compared to CTR that were

chondrocytes treated for the same period of time with 15% of the same culture medium used for lipoaspirate culture. Moreover, as shown in Fig. 9B, culture medium from the Col and LipoG batches activated ECM synthesis of chondrocytes, as shown by increased levels of GAGs.

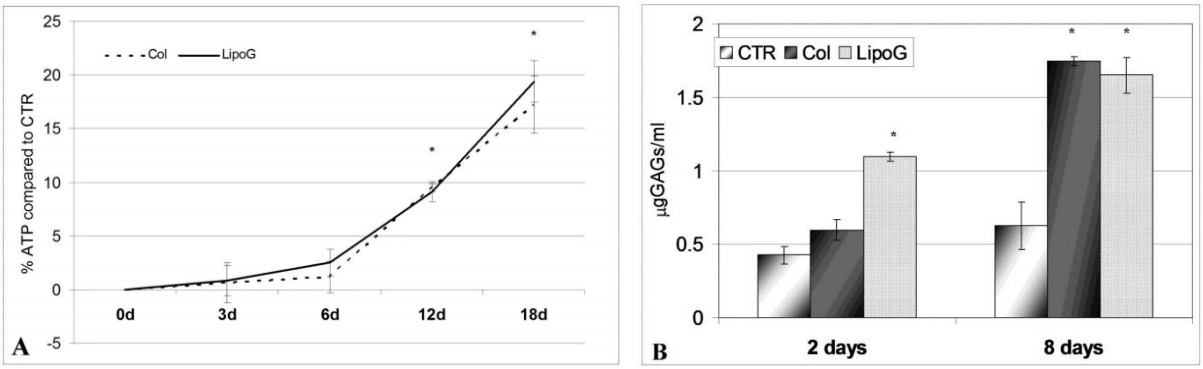

Figure 9: Proliferation (Figure 9A) and GAG production (Figure 9B) of human primary chondrocytes cultured with 15% of culture medium from lipoaspirates. Results in Figure 9A are expressed as mean ± SD relative to control cells (n=3); in Figure 9B results are reported as mean ± SD (n=3) in µg/ml of sulfated glycosaminoglycans quantified in culture medium of chondrocytes cultured for 2 days and 8 days in basal medium (CTR) and in culture media supplemented with 15% medium from lipoaspirates (Col and LipoG). *p<0.05 compared to CTR.

3.3.3 Cell outgrowth from lipoaspirates: quantification, phenotype, differentiation capacity, and cartilage repopulation.

The next stage of the research showed that the LipoG batch of lipoaspirate, when transferred into tissue culture, without any processing began to leave cells out from the tissue clusters after 2-3 days. Cells attached to the plastic of the tissue-culture wells and reached 70-80% confluence in 7-12 days. In Fig. 10 are reported representative images of cells grown out from the clusters: Fig. 10A showed cells at the bottom of the plastic wells which had grown out from the clusters when cultured in floating conditions; Fig. 10B showed cell outgrowth in the 3D collagen culture model. Both lipoaspirates (Col and LipoG) showed good cell outgrowth from the clusters; the

only difference was that, from the LipoG batch, outgrowth was faster than from the Col batch; further from the same weight of lipoaspirate, the number of cells from LipoG was higher than that from the Col batch. Of the two culture models studied, cell outgrowth was faster in the 3D collagen matrix than it was from the floating culture. Cell outgrowth was already visible within 2 days from time 0 in the 3D culture model, whereas no cells were visible before 4-5 days in the floating culture.

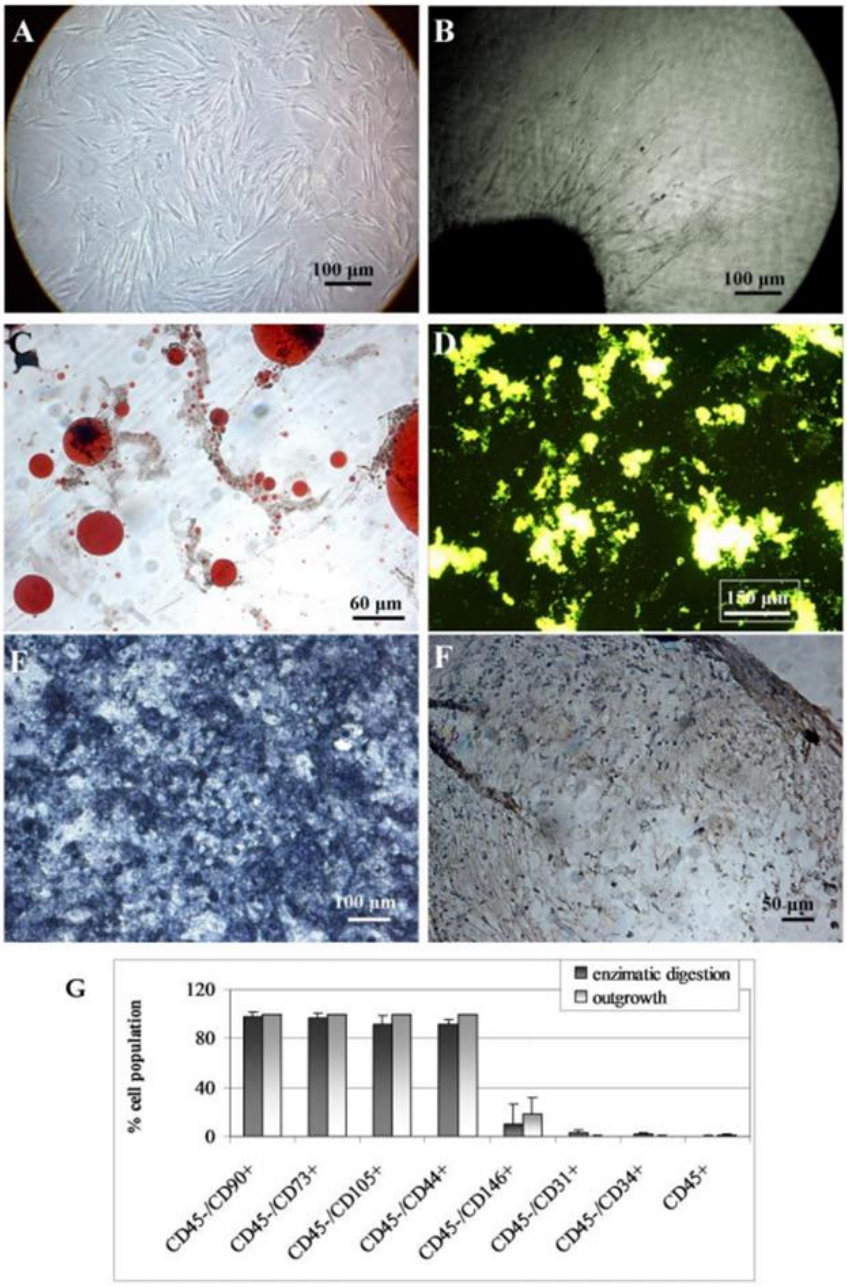

Figure 10: Cell outgrowth from clusters: representative images at phase contrast microscopy of cells outgrown from clusters in the monolayer culture model (Figure 10A) and in the 3D collagen matrix (Figure 10B). Figures 10C-F show representative microscopic images of four separate experiments of the multi-lineage differentiation capacity of the cells outgrowing from lipoaspirate. Adipogenic differentiation (Figure 10C) was revealed by Oil Red-O staining for neutral lipids. Osteogenic differentiation was evidenced by the formation of mineralized matrix as shown in green by Calcein staining in Figure 10D and ALP activity in Figure 10E. Chondrogenic differentiation was revealed by immune-histochemical stain for collagen II (Figure 10F). The bar-graph (Figure 10G) shows the immune-phenotyping flow cytometry analysis of cells expanded from the enzymatically digested lipoaspirate, and of cells outgrowing from cultured lipoaspirate. Data are expressed as means ± SD (n=3) of the percent of positive cells for the indicated markers.

FACS analyses (Fig. 10G) showed that cells obtained by outgrowth from the clusters expressed typical mesenchymal markers (CD90, CD73, CD105 and CD44) at high percentages, close to 100%, and also CD146 positive cells index of pericytes population Fig. 10 bar graph**.** No statistically-significant difference was found versus cells obtained by enzymatic digestion of the lipoaspirate. Furthermore, cells outgrown from the lipoaspirates were found to have the developmental potential of hMSCs (Fig. 10C-F). Adipogenic differentiation showed a progressive loss of the fibroblastoid-like shape, and the production of cytoplasm lipid vacuoles (Fig. 10C). Osteogenic differentiation was revealed at the first week of induction by morphological changes (from fibroblastoid-like to trapezoidal cells) and, at the end of the induction period, by the formation of mineralized matrix, as shown in Fig. 10D, and of ALP-positive cells (Fig. 10E). Chondrogenic induction revealed abundant extracellular matrix positive to human type II collagen antibody (Fig. 10F).

LVs were used to transduce cultured clusters of lipoaspirate. Transduction was visualized by GFP expression, and a very high transduction efficiency was demonstrated as shown by direct fluorescence (Fig. 11A). Transduction was not limited to the surface of the clusters, but was also evident in the inner part. Cell counts, performed with nuclear counterstaining, revealed that a mean of 62% ± 4% of cells of the cluster were GFP-positive, and no cell loss was detected (p=0.94 for comparison with control lipoaspirates, n=3). Moreover, 49±20% of cells outgrown from the lipoaspirate clusters were GFP-positive.

When GFP-transduced clusters were placed in an organ culture of healthy or mechanically-damaged cartilage, it was found that, within a few days, positive cells grew out from the clusters; moreover they only repopulated the damaged cartilage (Fig. 11C) and not its healthy counterpart (Fig. 11B). Among GFP-positive cells, only 10% showed SOX9 co-localization

indicating that, in the organ culture model used, only 10% of cells outgrowing from the lipoaspirate differentiated into chondrocytes (Fig. 11D).

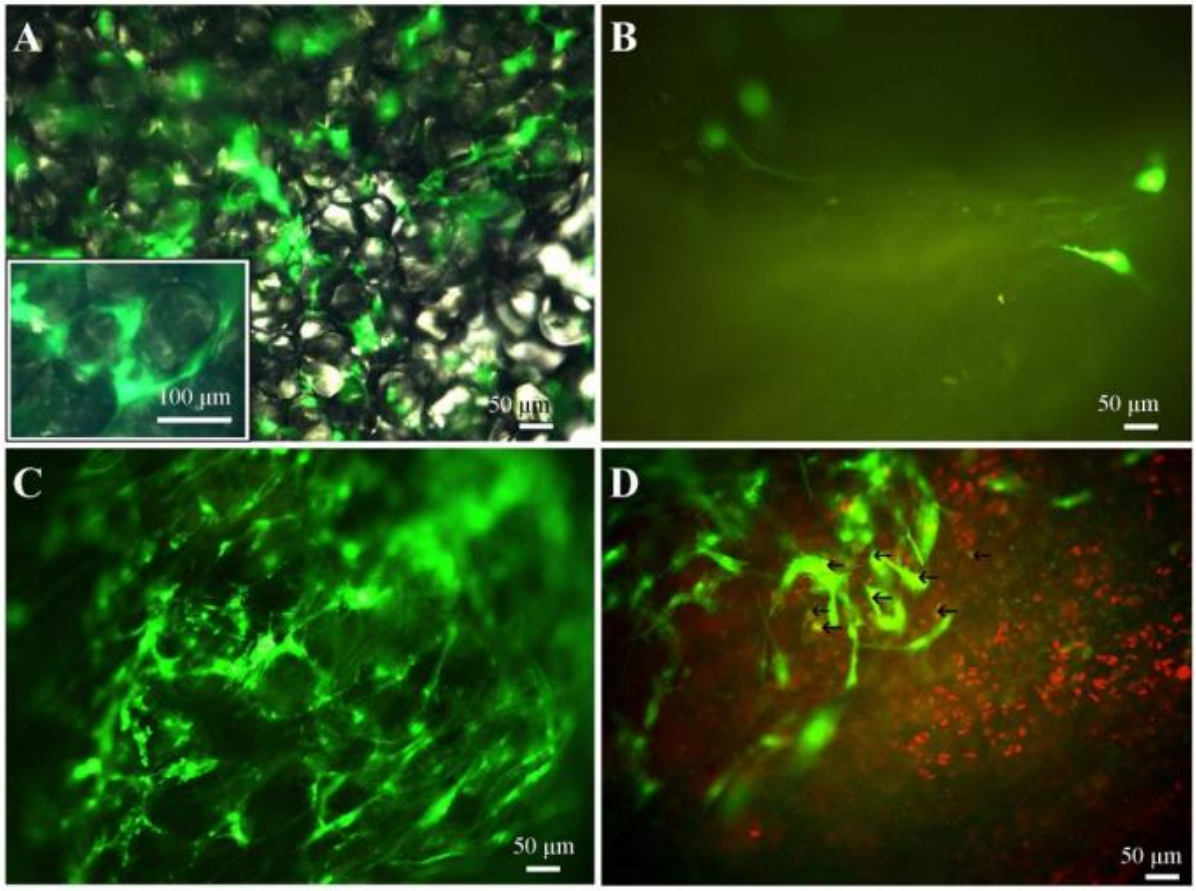

Figure 11: Lentiviral GFP transduction of the clusters is shown in Figure 11A. No GFP-positive cells growing out from GFP-transduced clusters are visible upon a healthy cartilage fragment (Figure 11B): a mechanically-damaged cartilage fragment was well repopulated (Figure 11C). Few of the cells that repopulated the damaged cartilage differentiated to chondrocytes (GFP-positive and SOX9-positive, yellow highlighted with arrows in Figure 11D).

3.4 Conclusions

The use of ASCs in regenerative medicine is a rapidly-growing area of research. There is some *in vitro* evidence of success using these cells in osteochondral defect repair (17), and they have also recently been used successfully as a therapeutic tool in treating OA (5). ASCs have been available commercially for veterinary use since 2003, although little has been published

documenting their clinical efficacy; such reports might minimize the gap between human and veterinary markets, accelerating the introduction of stem-cell-based cartilage repair for human diseases. Beneficial effects of ASCs have been reported in treating OA in some experimental animal models (19,33). However, these studies used a tissue-engineering approach, and a wide variety of biodegradable scaffolds were used to assist chondrogenic differentiation.

To our knowledge, use of an autologous biological tissue, naturally rich in stem cells, implanted in a different anatomical site from where it was harvested (i.e. autologous transplantation of subcutaneous fat to intra-articular sites) has not been previously attempted. The present study has shown that it is possible to avoid stem-cell isolation, expansion, and differentiation for several days *in vitro*, before autologous implantation with scaffold or scaffold-free approaches. We have demonstrated that micro-fragmented lipoaspirate clusters give rise to spontaneous cell outgrowth both when cultured in floating conditions and in the 3D collagen matrix. Although adipose tissue contains adipose-derived stem cells, fibroblasts, endothelial cells, hematogenous cells, pericytes, adipocytes, and pre-adipocytes, it was found that cells obtained naturally exhibit a mesenchymal phenotype with stem cell surface expression markers similar to those obtained through enzymatic extraction; they also have the capacity for multilineage differentiation, showing the classical commitment to osteogenic, chondrogenic and adipogenic lineages. These data show that micronized lipoaspirate, acting as a natural scaffold for mesenchymal cells that are simply trapped in the stromal vascular portion, may be considered a source of autologous multipotent undifferentiated cells. Since it requires no processing steps before use, the risk of infection, or that of retaining enzymatic residues from tissue digestion during cell isolation can be avoided. This also reduces costs associated with a long period of cell expansion and differentiation (12-21 days) with residual of growth supplements, as well as the side effects associated with the natural or synthetic scaffolds used for cell-based cartilage repair. Despite

these promising results, however, the physiological role of native adipose-derived stromal/stem cells *in vivo* is not fully understood, and more histological studies must be performed before it may be deemed safe for clinical use. It will be necessary to identify in situ the expression of a wide range of markers; these may well include more than those studied to analyze culture-expanded preparations (2). The use of GFP-transduced lipoaspirates demonstrated, *in vitro*, that cells outgrown from lipoaspirate can repopulate an organ culture of damaged cartilage. It may therefore be hypothesized that, when intra-articular injection of human lipoaspirate enters clinical trials, it will give rise to cells having mesenchymal potential to repopulate the lesion. Moreover, there appears to be a possibility that native stem-like cells arising from lipoaspirate, may have a better physiological phenotype and higher regenerative potential than cells obtained with the isolation technique and culture conditions generally used for ASC preparation prior to transplantation.

In addition to these data, the finding that lipoaspirate culture medium induced human primary chondrocyte proliferation and ECM synthesis reinforces the promise of such preparations, comprising micronized fat, becoming a therapeutic tool for cartilage regeneration. The paracrine and endocrine secretions of adipose tissue have recently been described (19); fat might not be considered only as an energy storage tissue, but rather as an active tissue involved in the metabolism (21), in immunomodulatory activities, and in providing an extensive peri-vascular reservoir of multipotent, undifferentiated cell populations, involved in homeostasis and regeneration. As a large micro-vascular bed, fat appears to provide an ideal pool of undifferentiated cells in close proximity to peri-vascular access routes for the mobilization and relocation demands of injured or diseased structures. It is characterized by different cell types (including adipocytes, pre-adipocytes, vascular cells, fibroblasts, pericytes, stem cells, and immune cells) that, by secreting a range of cytokines, growth factors, chemokines, and

adipokines, might interact with the resident cells of damaged tissue, inducing repair and regeneration. As for ASC preparations, which are already in clinical trials, many questions remain to be clarified concerning lipoaspirate differentiation potential *in vivo*, and the mechanisms involved in repair or regeneration (paracrine effects, differentiation, immunomodulation), together with any donor-specific variability in cell quality and activity.

In an attempt to determine the fate of lipoaspirate when injected into a joint, it was induced to differentiate *in vitro* to form cartilage, as has generally been done using MSCs in a 3D culture model (6). Micronized fat (LipoG) responds better to differentiating stimuli than did the other batches, which contained clusters of larger size; this may be because the more micronized clusters have a greater surface area in contact with the culture medium containing chGF, giving the cells a greater response capacity. Based on these findings, it might be hypothesized that, when injected intra-articularly, lipoaspirate might become a fibrous tissue, having favorable mechanical, morphological, biochemical, and molecular characteristics for its use at intra-articular sites. At *in vitro* examination, an abnormal change in the nature of the adipose tissue was seen to have occurred, with residual fat globules surrounded by thick fibrous tissue rich in collagen and GAG that was reminiscent of metaplasia. Although the newly-formed tissue was not hyaline cartilage, as demonstrated by the lack of expression of type II collagen, it showed histological features and mechanical properties that in the joints, where the cartilage is damaged, would undoubtedly be superior to the classic viscosupplements used to alleviate the load acting on damaged cartilage. The fibrous intra-articular sleeve produced by the lipoaspirate preparation, by helping to support the load upon the injured articular heads, could provide a protective action on resident chondrocytes, which being less stressed would be stimulated to regenerate, leading to repair of the damaged tissue.

In conclusion, intra-articular injection of lipoaspirate may be considered a possible strategy to resolve lesions to the cartilage. This possibility shows promise for the production of a new generation of active injectable scaffolds (made of autologous tissue requiring no preparation steps) which could help clinicians to treat focal cartilage defects and osteochondral defects, using lipoaspirate from the patient to be treated. The use of human materials for transplantation (cells, tissues, and organs) is not without risks that may be related to the donor, the process of relocating the tissue from donor to the patient or depend to the condition of the receiver. In the application proposed in this study, since lipoaspirate was autologous, there would be no risk of rejection, or of transmitting disease from donor to recipient; further, there would be no need for procurement, processing, testing, storage, or quality control. Some limitations must be overcome before this procedure could enter widespread use, such as short- and long-term unpredictability, in-vivo intra-articular performance, and the fate of cells outgrown from lipoaspirate and of the lipoaspirate itself (bio-distribution).

Lipoaspirate and Lipogems® are both minimally-manipulated autologous materials, not combined with other products, and intended for homologous use; they are therefore classified as HCT/Ps in section 361 of the Public Health Service Act and FDA approved for clinical trials. For these reasons, the therapeutic approach is possible yet even if only clinical results will demonstrate its safety (ruling out inflammatory reactions, fibrosis, mal-differentiation, and any tumorigenic activity) and further studies are needed to demonstrate its efficacy that might be dependent on age, body mass index, gender, ethnicity, existing diseases, or other factors.

4. Bone regeneration

4.1 Introduction

The aim of regenerative medicine is to replace and repair lost or damaged tissues stimulating the natural regeneration process (38). In bone regeneration, the gap between the damaged bone fragments has to be filled with functional materials that act as a substrate and as a physical three-dimensional microenvironment able to induce the migration of cells from the native tissue, to organize cells and to provide differentiation and maturation signals that positively promote osteogenesis (75).

The ability of a substrate to favor hOB and hMSC migration, proliferation and differentiation corresponds to the ideal characteristics of a material for bone tissue regeneration. It can be obtained using a medicated scaffold which provides an extracellular matrix-like environment that facilitate cell migration and proliferation of resident osteoblasts and mesenchymal cells from the margin of the defect and favor their differentiation to form new bone in the defect area. Some studies propose modifications of the scaffolds with one (76) or more (77-79) categories of bioactive molecules to improve cell adhesion, osteoconduction and osteoinduction to achieve better osteointegration.

It has never been thought to the possibility to exploit cell mediated contraction of a 3D gel scaffold to expedite the approach of the bone fragments and bone regeneration even if recently it has been hypothesized that the contraction capacity of osteoblasts may play an important role in forming bridges between fragments of fractured bone (80) or imparting an architecture during bone remodelling (81). The bioactive lipid LPA has recently emerged as highly significant regulator of bone cell biology by inducing osteoblast chemotaxis (82), growth (83), maturation

(84) and survival (85), by promoting dendrite outgrowth in osteocytes (86) and by stimulating osteoblastic differentiation of hMSC (76). Moreover, by triggering actin stress fibre accumulation and cytoskeletal reorganisation, LPA could stimulate collagen matrix contraction with the approach of bone fragments. For these reasons we have decided to use LPA to functionalize injectable extracellular matrix scaffold that is able to reduce the time required for fracture healing and speed bone regeneration in bone deficiencies such as non-unions or sinus lift augmentation. When injected in the bone defect it probably act as substrate that cells from the damaged tissue can attach and populate by proliferating into and migrating across and then reorganize the matrix transforming it into new bone. To study these hypothesis we have developed a 3D collagen gel, generally used to demonstrate the mechanisms by which cells contract but only recently considered as potentially useful biological tool containing growth factors for 3D bone tissue engineering (87). We have tested if LPA enriched collagen could act by modulating gel contraction rate and bone regeneration when used alone or mixed with 1,25D3 that is known to synergistically co-operate with LPA on osteoblast maturation (84,88). The effect of LPA on hOB in a collagen gel scaffold have been studied in order to evaluate if it was possible to increase osteoconductivity and osteoinductivity in view of bone tissue engineering application.

4.1.1 Bone tissue

The bone tissue is one of the connective tissues with support function. As each connective tissue, bone tissue contains specialized cells and an extracellular matrix composed of fibers of proteic nature and fundamental substance. The matrix of the bone tissue is solid and durable due to the deposition of calcium salts around the fibers. The extracellular matrix of bone tissue is

composed largely of calcium phosphate, $Ca_3(PO_4)_2$ that interacts with the calcium hydroxide $Ca(OH)_2$ to form hydroxyapatite crystals, $Ca_{10}(PO_4)_6(OH)_2$. Newly formed, these crystals incorporate other calcium salts, such as calcium carbonate and ions such as sodium, magnesium and fluoride. The remaining part consists of organic fibers highly ordered, constituted for 90% by collagen (of this, 97% is type I and 3% is type V), by numerous non-collagenous proteins (osteocalcin, osteonectin, osteopontin, fibronectin, thrombospondin, sialoproteine, proteoglycans, biglycan, albumin and immunoglobulins) and water. The inorganic mineral component gives to the tissue remarkable mechanical properties such as hardness and resistance to compression; while the composition and distribution of the protein components of the matrix gives elasticity and resistance to fracture. In particular, collagen I has a tertiary structure characterized by spiral winding of three identical polypeptide chains that are repeated sequences of aminoacids uncommon into proteins (proline, glycine, hydroxyproline and hydroxylysine), and is this structure that confers the elastic properties to the molecule, and then to the tissue.

The cellular component of the bone tissue is characterized by three types of cells: osteoblasts, which generate bone matrix, osteocytes, which possess metabolic activity and osteoclasts that degrade the bone matrix. The balance between the activity of osteoblasts and osteoclasts is very important to maintain skeletal homeostasis.

From the histological point of view we can divide the bone tissue in: spongy and compact bone tissue. The compact bone is relatively solid and usually form the walls of the bones. The functional unit of compact bone is the osteon, formed in turn by concentric lamellae, which are aligned parallel to the longitudinal axis of the bone. The concentric lamellae form a series of concentric rings around the central channel and the collagen fibers are distributed in a spiral along the axis of each blade. Spongy bone form a network of trabeculae and laminae, surrounds the medullary cavity which contains the bone marrow, a connective tissue in which can prevail

adipocytes (yellow marrow) or a mixture of red and white blood cells and stem cells (red marrow). The lamellae in this tissue form the trabeculae and there are a number of free spaces between the trabeculae. The branching of trabeculae gives to the bone a considerable resistance when compared to the weight.

The bone is covered externally by a lamina of connective tissue called periosteum that insulates and protects the bone from the surrounding tissues. The periosteum is constituted by a fibrous outer layer of dense connective tissue and an inner layer containing the progenitor cells: mesenchymal cells that can generate daughter cells able to differentiate into osteoblasts (the ability to produce new osteoblasts is very important after a bone fracture). The periosteum is not present in the points of attachment of tendons, ligaments and joints and at points where the bones are covered with cartilage.

On the inner surface of the bone, the medullary cavity is coated by endosteum. This layer that contains progenitor cells, osteoblasts and osteoclasts covers the trabeculae of cancellous bone and lines the inner surface of the central channel and piercing channels (78).

4.1.2 Bone healing

Fracture healing is a complex but well orchestrated regenerative process initiated in response to injury, resulting in optimal skeletal repair and restoration of skeletal function. It involves the coordinated participation of haematopoietic and immune cells within the bone marrow in conjunction with vascular and skeletal cell precursors, including MSCs. Multiple factors regulate this cascade of molecular events by affecting different sites in the osteoblast through different processes such as migration, proliferation, chemotaxis, differentiation, inhibition and extracellular protein synthesis (82).

After fractures there is the hematoma formation, fueled by the breaking of the periosteal and endosteal vessels. An inflammatory response occurs with the recruitment of macrophage cells, white blood cells and mesenchymal stem cells that differentiate into chondroblasts and osteoblast. In this phase chondroblasts form hyaline cartilage and osteoblasts form bone tissue (Figure 12).

These two new tissues grow in size until they unite with their counterparts from other sides of fracture. These processes culminate in a new mass of heterogeneous tissue which is known as the fracture callus. Eventually, the fracture gap is bridged by the hyaline cartilage and bone tissue, restoring some of its original strength. The next phase is the replacement of the hyaline cartilage and bone tissue with lamellar bone. The replacement process is known as endochondral ossification. The lamellar bone begins forming soon after the collagen matrix of either tissue becomes mineralized. The osteoblasts form new lamellar bone upon the recently exposed surface of the mineralized matrix. This primary bone formation is followed by remodeling in order to obtain the final structure and regain the primitive mechanical strength (83).

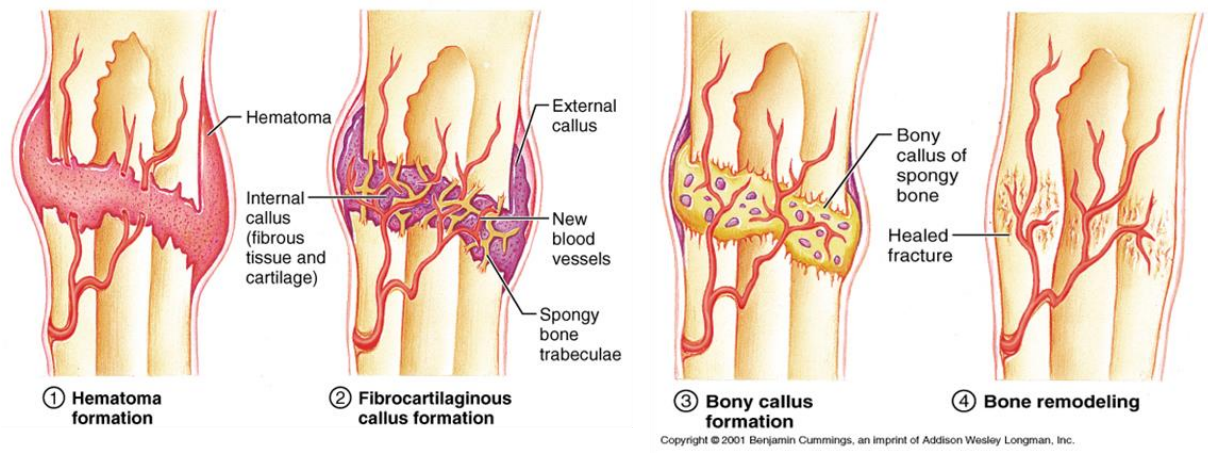

Figure 12: The Process of Fracture Repair. The healing of a bone fracture follows a series of progressive steps: (1) A fracture hematoma forms. (2) Internal and external calli form. (3) Cartilage of the calli is replaced by trabecular bone. (4) Remodeling occurs.

4.1.3 Bone regeneration

Bone regeneration is required in the treatment of many orthopedic diseases (osteoarthritis of the hip, knee osteoarthritis and meniscus tear) and for repairing defects of compact bone and spongy bone as a consequence of trauma, congenital malformations or tumors both in the orthopedic field and in the field of maxillofacial surgery.

In reconstructive surgery, there is an increasing demand for replacement material to fill defects especially in bone and cartilage. Usually, implants made of synthetic polymers, ceramics and metals, as well as transplants made of tissue derivates such as collagen or fixed cartilage allografts, are used for tissue repair. However, none of these materials can provide the quality of the original tissue. These artificial materials often fracture, induce immunological responses and are difficult to anchor, in contrast with vital tissues they lack any process of regeneration. Thus, the goal of tissue repair is the autologous growth or regeneration of the original tissue without remnants of foreign biomaterials (88). In order to regenerate the tissue, it must realized three-dimensional structures capable of inducing stimuli adapted to tissue growth. In fact, many studies show that isolated cells are unlikely able to organize themselves spontaneously to form complex tissues in the absence of a three-dimensional structure that will guide and stimulate the activity. Normally cultured cells are able to multiply and to proliferate only in two dimensions. Therefore, tissue regeneration needs cells, scaffold and growth factors: the cells synthesize matrices of new tissue, the scaffold provides the appropriate environment for cells to be able to effectively accomplish their missions and mimics the function of the extracellular matrix, and the function of growth factors is to facilitate and promote cells to generate new tissue (89). This means that, in physiological environment, the presence of the implant and its degradation must

induce and maintain conditions that positively influence cells survival, proliferation and deposition of extracellular matrix (90).

Important parameters for design a scaffold are: the degree of porosity (pore number, pore size and interconnections of pores), the chemical composition (for example the presence of osteoinductive materials such as hydroxyapatite or tricalcium-phoshate), the degradation or resorption rate and mechanical properties. Scaffolds may be of natural origin, synthetic or hybrid. Those of natural origin include bone substitutes of human or animal origin. These are: autografts (autologous bone taken from the iliac crest or ribs of the patient), allografts (human bone obtained from a donor; these carry the risk of disease transmission and host immune response) and xenografts (tissues taken from animals, which are the most commonly used but they carry greater risk of immune rejection, in situ degeneration and disease transmission) (91). Synthetic scaffolds are obtained by modifying polymers, ceramics or metals, which can be resorbed or not. Hybrid scaffolds are collagen-based structures with the addition of synthetic polymers or minerals such as hydroxyapatite: these scaffolds try to mimic perfectly the original mineralized bone matrix. In the choice of material and the structure's design process of the scaffold, the nature of the skeletal defect and the mechanical strength which will be submitted to the replaced bone portion must be assessed. Structural properties in fact determine the mechanical responses, such as elasticity and resistance to compression, typical of compact bone, or the ability to withstand and to transmit load forces, property of the cancellous bone. Collagen has characteristic properties of a biomaterial, such as biocompatibility, biodegradability, ductile properties (ease of processing and the possibility of sterilization). Also, it has chemical characteristic (composition) and physical properties (mechanical properties and porosity) that are compatible with its use as a scaffold.

Collagen is biocompatible with the physiological environment and the cells, both *in vitro* and *in vivo*, it is a material able to stimulate adhesion, proliferation and cell differentiation, thus favoring the regeneration and integration into existing bone, so it can be an ideal bone substitute. Collagen is also a main component of the extracellular matrix and thus it provides a substrate well accepted by the cells and able to transmit signals to the cells. The extracellular matrix is not just a support system, but it is extremely important in intercellular communication. The cells are sensitive to the mechanical strength of the extracellular matrix which they respond to, with changes in cytoskeleton, thorough interaction with integrins, but also slight changes in the topographical fibrillar organization and chemical composition of the matrix may be translated to growth stimuli, differentiation and cell motility. The substrates that mimic the ECM have also to be able to lead the cells towards differentiation.

4.1.4 Cellular morphological changes and Rho pathway

In response to environmental signals, a cell changes both its shape and its degree of attachment to the substratum. These changes are caused, at least in part, by rearrangements of the cytoskeleton. The cytoskeleton is a organized structural system composed of different types of filaments: actin filaments (6-10nm diameter), intermediate filaments (7-11nm) and microtubules (25nm). The mechanical properties of the cytoskeleton play a key role not only in determining the cell shape, but also in other function such as: spreading, migration, orientation ad cytokinesis. The cytoskeletal remodeling is inhibited by depolymerization of microtubules and also has been shown that the activity of tyrosine-kinases receptors and intracellular calcium levels play a key role in this mechanism of remodeling.

At the molecular level, the rearrangement of the cytoskeleton is controlled in large part by a family of proteins with GTPase activity, Rho protein.

Rho is a small GTPase, which exhibits both GDP/GTP binding and GTPase activities. Rho has GDP-bound inactive and GTP-bound active forms, which are interconvertible by GDP/GTP exchange and GTPase reactions (92).

Rho is implicated in the cytoskeletal responses to extracellular signals including lysophosphatidic acid and certain growth factors, which form stress fibers and cause focal adhesion. Rho is also implicated in other physiological functions associated with cytoskeletal rearrangements such as cell morphology, cell aggregation, cell motility, and cytokinesis. More studies indicate that Rho is also involved in the regulation of phosphatidylinositol 3-kinase (93), phosphatidylinositol 4-phosphate-5-kinase (94), and c-*fos* expression (95). The most important members of the family of Rho GTPase are: Rac1, RhoA and Cdc42. The activation of Rho induces primarily the polymerization of actin and myosin, whereas Rac and Cdc promote mainly the formation of cytoplasmic protrusions, such as lamellipodia and filopodia (97).

Each Rho protein affects numerous proteins downstream, all of which have roles in various cell processes. In fact, over 60 targets of the three common Rho GTPases have been found (98).

A serine/treonine kinase associated at RhoA protein is Rho-associated coiled-coil-containing protein kinase (ROCK) (99). It is mainly involved in regulating the shape and movement of cells by acting on the cytoskeleton. Different substrates can be phosphorylated by ROCKs, including LIM kinase, myosin light chain (MLC) and MLC phosphatase. These substrates, once phosphorylated, regulate actin filament organisation and contractility as follows:

- ROCK inhibits the depolymerisation of actin filaments indirectly: ROCK phosphorylates and activates LIM kinase, which in turn phosphorylates ADF/cofilin, thereby inactivating its

actin-depolymerization activity. This results in the stabilization of actin filaments and an increase in their numbers. Thus, over time actin monomers that are needed to continue actin polymerization for migration become limited. The increased stable actin filaments and the loss of actin monomers contribute to a reduction of cell migration (100).

- ROCK also regulates cell migration by promoting cellular contraction and thus cell-substratum contacts. ROCK increases the activity of the motor protein myosin II by two different mechanisms. Firstly, phosphorylation of the myosin light chain (MLC) increases the myosin II ATPase activity. Phosphorylation of MLC has been shown to induce a conformational change in myosin, thereby increasing its binding to actin filaments and subsequently the formation of stress fiber (101). Secondly, ROCK inactivates MLC phosphatase, leading to increased levels of phosphorylated MLC. Thus in both cases, ROCK activation by Rho induces the formation of actin stress fibers, actin filament bundles of opposing polarity, containing myosin II, tropomyosin, caldesmon and MLC-kinase, and consequently of focal contacts, which are immature integrin-based adhesion points with the extracellular substrate (102) (Figure13).

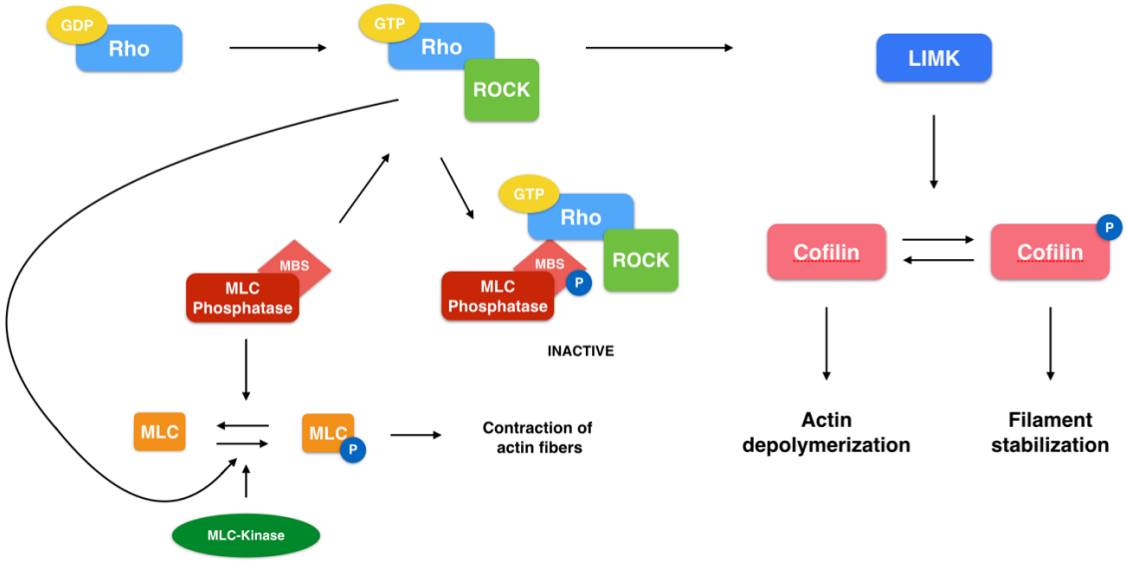

Figure 13: The RhoA/Rho-kinase signaling pathway. Active RhoA in GTP-bound conformation interact with Rho-kinase. Rho-kinase (ROCK) phosphorylates MLC phosphatase, inactivating it and also ROCK phosphorylates MLC, that induce a conformational change in myosin. ROCK actives also LIMK that phosphorylates cofilin. The phosphorylated cofilin is inactive and therefore allows actin filaments to stabilize.

The myosin has a role in motor activity along the actin filaments and it is important in the formation of cytoplasmic processes such as filopodia. In a study of morphological changes of the cytoskeleton in 3D cultured osteoblast is viewed as, line osteoblast MC3T3-E1 have an abundant distribution of myosin in cellular processes, suggesting a hight motor activity in collagen gel (103). The hypothesis is also supported by another study on dendritic process of fibroblast in 3D culture, where these were defined as dynamic structures undergoing stages of elongation and contraction, and these changes are led always by the Rho protein (104).

4.1.5 Lysophosphatidic acid (LPA)

Lysophosphatidic acid (LPA) is a phospholipid mediator with pleiotropic growth factor properties that elicit its actions via the activation of G protein-coupled receptors encoded by the

endothelial differentiation gene family (105). Lysophosphatidic acid (LPA) is a glycerophospholipd composed of a fatty acyl chain, glycerol backbone and a phosphate head group and it is biologically active on different cell types such as endothelial cells, fibroblast and cells of the bone tissue. This phospholipid is mainly produced by the following pathways. The generation of lysophospholipids (LPLs) for their subsequent conversion to LPA is one of the main mechanism. In the instance PLA1 (phospholipase A1) and PLA2 generates LPLs which serve as substrate for autotaxin (ATX), a member of the ectonucleotide pyrophosphatase/ phosphodiesterase family that exhibits unique lysophospholipase D activity allowing for the conversion of LPLs into LPA (106). Another source of LPA is cell membrane phospholipid metabolism to phosphatidic acids via the actions of phospholipase D, PA are subsequently converted to LPA by PLA1 and PLA2.

LPA, predominantly bound to serum albumin, is present in plasma at 0.5 - 1.0 μM and it is produced by the degranulation of platelets during clot formation. LPA is produced de novo by platelets when they are stimulated by prothrombotic factors (such as thrombin), so it is not accumulated, and its production is always meditated by autotaxin, that is present in serum at the concentration of ～100nM (107).

LPA is also produced by osteoblast that express multiple subtypes of P2X and P2Y receptors. Particularly they express P2X7 receptor that have been implicated in skeletal remodeling and mechanotransduction and it leads to production of LPA. It has been shown that by stimulating cells with BzATP, agonist of P2X7, there is a rise in the production of LPA through the sequential activation of PLD and PLA2. This observation suggests that probably LPA, produced by osteoblasts, acts in autocrine manner to regulate themselves and also it acts as a paracrine factor to regulate the activity of osteoclasts (108).

At present 7 cell surface receptors for LPA have been found. Of these LPA receptors 1-4 appear to be the most significant for skeletal cells. Each one is of the serpentine, seven transmembrane domain GPCR type. LPA receptors 1-3 inhibit adenylate cyclase but activate phosphoinositide 3-kinase (PI3K) and mitogen-activated protein kinase (MAPK) via coupling to $G_{\alpha i}$. These receptors are also known to couple to $G_{\alpha q/11}$ leading to PKC activation and increased intracellular calcium (iCa^{2+}) mobilization. LPA 1 and 2 are also coupled to $G_{\alpha 12/13}$ culminating in cytoskeletal reorganization via Rho/Rho kinase (ROCK) pathways (109) (Figure 14).

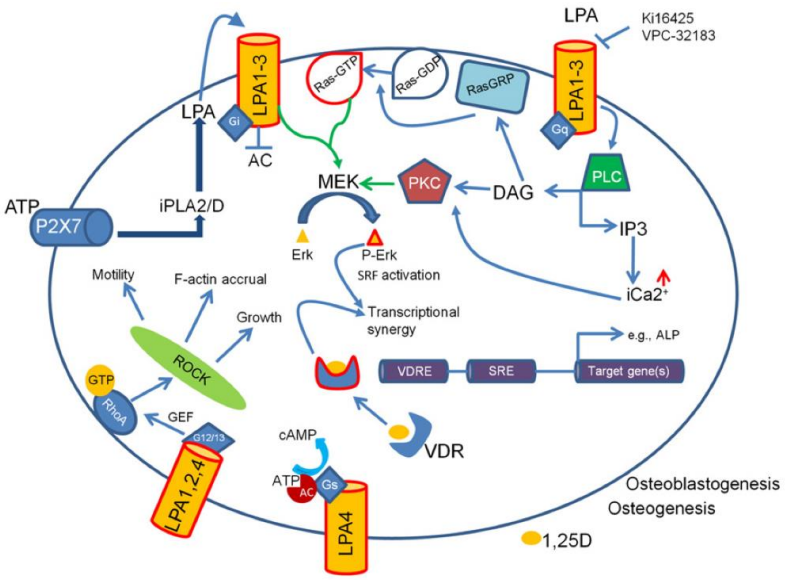

Figure 14: Multiple LPA GPCRs are associated with osteoblast; G_i, G_q, and $G_{12/13}$ coupled receptors are LPA receptors 1-3, whereas G_s is coupled to LPA4. Each receptor is allied to different downstream effectors. In this image there is also a synergic pathway with 1,25D. The synergy in proliferation for example is probably a consequence of transcriptional co-operation.

As already said, LPA is known to affect a wide variety of cell types, but, because the production of this lipid was associated with blood clotting and wound repair, many studies had focused on endothelial cells. LPA stimulates endothelial cell migration and may be a critical angiogenetic factor during wound healing (110). During bone fracture healing, platelets trigger the formation of blood clots that subsequently are replaced in a stepwise manner with mineralized tissue and

lysophospholipids may modulate osteoblast during bone repair (111). In more recent articles LPA induces proliferation and differentiation on human osteosarcoma cell lines (112), increases intracellular Ca^{2+} and cAMP levels (113) and induces ERK phosphorylation (114). LPA also induces chemotaxis in MC3T3-E1 osteoblastic cells, increasing both the average cell migration distance and migration velocity (115). Also the cytoskeleton reorganization of MG63 cells is affected by the action of LPA, which increases actin stress fiber formation. In this study the architectural changes induced by LPA are compared with cells treated with colchicine, a microtubule-disrupting agent known to generate actin stress fibers and the results were similar, but certainly cells treated with LPA presented morphological changes less dramatic than cells treated with colchicine (116).

LPA is also shown to be able to induce osteogenesis of hMSC, as demonstrated by LPA dose/dependent increase of matrix mineralization. For this analysis cells were seeded in differentiation medium, supplemented with ascorbic acid and β-glycerophosphate, with or without LPA (117). Moreover there are evidences that the use of LPA bound to albumin raises total ALP and matrix calcification in long-term (3 weeks) treated hMSC cultures, in contrast to the action of free LPA. Albumin is a natural carrier of LPA and LPA in association with albumin remains bioactive and can even heighten the cell response to this lysophospholipid (118). The use of albumin-bound LPA (HSA) will afford a much greater lifespan of the lipid by providing resistance to lipase action which may be one explanation for the greater efficacy of HSA over free LPA for the long term cultures. Importantly the use of LPA as a complex with albumin would appear to be important for promoting osteoblast formation from stromal cells. When hMSCs were co-treated with HSA and D3 in the presence of Ki16425 (LPA receptor antagonist) no increase in total ALP occurred, thus confirming that elevated enzyme activity was a consequence of the LPA bound to albumin (119). It confirms also that the co-treatment with

LPA and D3 is better than the treatment with only LPA or only D3, that act in a synergistic manner.

LPA produces an increase in the Rho-kinase activity in fibroblastic cells in 3D cultures and causes the retraction of cellular extensions and as a result it causes a contraction of the matrix. This change induced by LPA in the dendritic network can be blocked with an inhibitor of Rho-kinase (120).

It has been also studied the activity of LPA as an exogenous cell-traction inducing agent to remodel the ECM using articular chondrocytes and meniscus cells. LPA treated chondrocytes and meniscus cells contracted in size, retracting their filamentous actin cytoskeleton and any cell extensions or processes. Additionally LPA-treated tissue (self-assembling fibrocartilage construct) displayed greater staining under polarized light, indicating an increase in collagen alignment and/or density and it present enhanced tensile properties. This study demonstrates the promotion of cell traction forces and concomitant cytoskeleton contraction as a beneficial strategy in tissue engineering. No change in collagen content accompanied this effect, implicating that an increase in collagen organization was responsible for the enhanced tensile properties. ECM organization is essential to mechanical strength and stiffness in collagen-rich tissues. The increase in ECM organization might be accelerated by an increase in cytoskeletal reorganization. Indeed, when treated with LPA, articular chondrocytes and meniscus cells displayed significant cytoskeletal contraction, leading to retraction of cell extensions or processes, rounder cell morphology, and decreased cell size (121) (Figure 15).

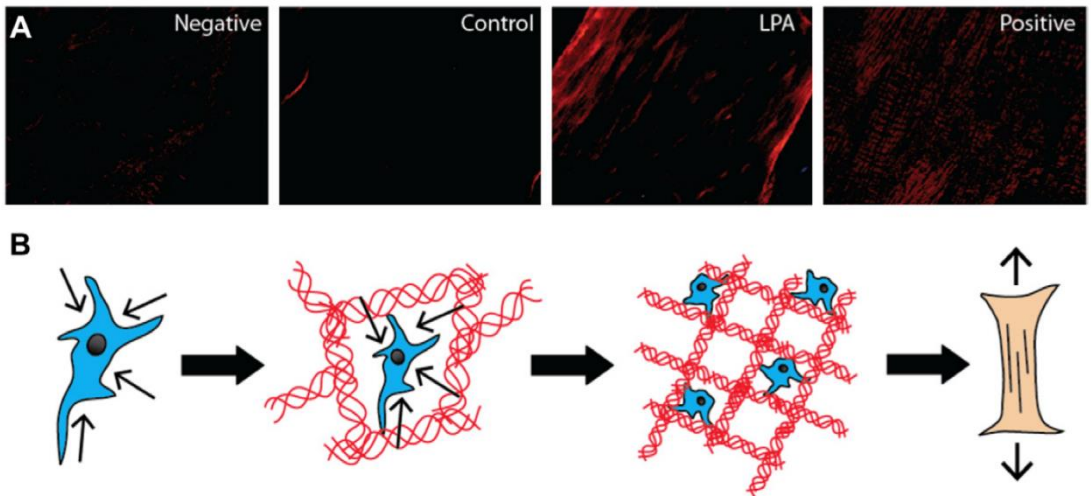

Figure 15: Organization of ECM collagen. (A) Polarized light microscopy of native muscle, control construct, and native meniscus fibrocartilage, showing increasing collagen alignment and/or density. (B) Schematic of possible mechanism by which LPA increases tensile properties of engineered tissue. Cytoskeletal contraction results in cell traction on the ECM, leading to remodeling of the collagen network and an increase in ECM alignment.

4.2 Materials and methods

4.2.1 Cell culture and reagents

Human primary osteoblast (hOB) were obtained from human trabecular bone fragments (taken at surgery after informed consent and provided by the Orthopedic Institute, Major Hospital, Novara, Italy). Bone fragments were treated for 30 minutes at 37°C under stirring, with a mixture of bacterial protease enriched with collagenase: bacterial collagenase 3 mg/ml, 6.5 U/ml elastase, 18.22 mg/ml D-sorbitol, 6 mg/ml chondroitin sulfate (Sigma) dissolved in Kreb's IIA buffer (111.2 mM NaCl, 21.3 mM Tris base, 13.0 mM glucose, 5.4 mM KCl, 1.3 mM $MgCl_2$, 0.5 mM $ZnCl_2$, pH 7.40).

Bone fragments were put in plate with Iscove's modified Dulbecco's medium (IMDM, Euroclone) supplemented with 20% foetal calf serum (Hyclone, USA), 2mM L-glutamine, and antibiotics. The spillage of the cells from the bone fragments was visible after a week and the

cells reach confluence after 3-4 weeks. After removal of the fragments, the cells at confluence were trypsinized and were put in new plates of the cell culture, the medium was the same but with 10% of FBS. Cells from up to five passages were used for all the experiments. For the cultures in the presence of the compounds to be tested cells were starved for 24 hours and cultured in serum free media supplemented with 250 µg/mL essentially fatty acid free human serum albumin (FAFA) containing either D3 (final concentration of 100 nM) or LPA (1 µM) or a combination of both. FAFA is used because albumin is the natural carrier for LPA, furthermore albumin-bound LPA is known to improve the cell response to this lipid (118). Where not specified reagents were form Sigma. Stocks of D3 were prepared in ethanol (1 mM) and stored at -20°C. Stocks of LPA were prepared in PBS (10mM) and stored at -20°C.

4.2.2 Isolation of collagen from rat tails

Collagen was isolated from the tendons of rat tails in according to (122). After removing the skin the vertebrae has been broken starting from the tip and the visible tendons were removed, tendons should be white and as clean as possible. It operates in the same way for the entire length of the tail. The tendons isolated were left to dry in air for 3-4 hours. The tendons were then dry weighed and subsequently sterilized with ultra-violet lamp for 48 hours. The sterile tendons were transferred to a sterile solution of 0,1% acetic acid at a concentration of 300 ml/g of tendons. The extraction of collagen requires stirring for 24 hours in the cold room at 4°C. At the end we obtain a solution composed of collagen and undissolved fibers, these latter were eliminated by filtration on sterile gauze. Final solution contains 2 mg/mL of soluble collagen as estimated from BCA (BCA Protein Assay kit, Pierce) and Sirius Red assay according to (123). Briefly, 100µL of rat tail collagen or of standard collagen were air dried and stained with 1 ml

Sirius Red dye reagent (1mg/ml in saturated aqueous picric acid) for 1 h. The dye solution was removed, washed with 0.01 N hydrochloric acid to remove all non-bound dye and the stained material dissolved in 0.2–0.3 ml 0.1 N sodium hydroxide measured with a BioRad microplate reader 3550 at 550 nm against 0.1 N sodium hydroxide as blank. The results were reported as mean ± SD (n=3) μg collagen/ml.

4.2.3 Silver Staining in acrylamide gels

To obtain a qualitative and semiquantitative indication on collagen has been carried out electrophoresis on an acrylamide gel in the presence of sodium dodecyl sulfate (SDS-PAGE). Collagen isolated was loaded on polyacrylamide gel. Proteins can be highlighted directly on the gel by staining with silver nitrate, coloring performed with the Silver Stain kit (Fermentas) is based on the fact that the silver nitrate reacts with the binding sites of the protein in acid. Subsequently, the silver ions are reduced to metallic silver due to oxidation of formaldehyde in alkaline conditions. The sodium carbonate buffers the formic acid product from the oxidation of formaldehyde, so that the reduction of silver ions may continue until the protein band on the gel appears.

4.2.4 Collagen matrix contraction

Osteoblasts in FAFA-IMDM without serum were mixed at a ratio 1:1 in the collagen solution prior to gel formation at different cell densities to understand if gel contraction was cell mediated and if it was cell concentration mediated. The range of hOB concentration studied was: 10^2 cells/ml, 10^3 cells/ml, 10^4 cells/ml, 10^5 cells/ml, 10^6 cells/ml and 10^7 cells/ml. A density of $5x10^4$ cells per 100 μl gel was used to test the activities of 1,25D3 (10^{-7}M) and LPA (1 μM) or

the combination of both on collagen contraction. Cell/collagen mixture cultured without D3 or LPA was used as basal control while aliquots added with Y27632 (10 μM), a Rho kinase antagonist, were used to understand if the contraction was ROCK mediated. Each aliquot occupied an area outlined by an 10 mm diameter circular score within a well. Polymerization of collagen matrices requires 60 min at 37°C. Subsequently the polymerized matrices were cultured with 1 ml of FAFA-IMDM added with the factor to be tested that were added also in culture media every 3 days. Triplicate samples were analyzed and the experiment was repeated three times.

To determine the extent of matrix contraction two methods were used: 1) the matrices were measured and contraction data presented as the change in diameter (starting-final); 2) two fragments of decellularized human spongiosa (Puros, Zimmer) have been put inside each gel before polymerization and the change in distance between the fragments was measured during the experiment. At time 0, 1 hour, 1, 3, 6, 12 and 24 days images of the gels were taken and distances from the bone fragments quantified. Measures were done using an inverted microscope equipped with a digital camera connected to an image analysis system (all from Leica Microsystems).

4.2.5 Fluorescence and confocal microscopy

The 3D collagen cultures after 24 hours of treatments or cultures on coverslips were fixed for 20 min at room temperature with 3% paraformaldehyde in PBS, blocked with 1% glycine and 1% bovine serum albumin in PBS for 30 min, and permeabilized with 0.2% Nonidet P-40 in PBS for 10 min. To stain for actin, samples were incubated with rhodamine-conjugated phalloidin (8 units/ml) or Alexa fluorescent Phalloidin (Fluor A12379 488-green Invitrogen

1:40 in BSA) overnight in the dark. For the staining of myosin as actin-binding protein, important in motor activity along actin filaments in contractile bundles, samples were incubated with anti-Myosin light chains (Sigma, 1:200) overnight at 4°C and then with secondary antibody conjugated to fluorescein isothiocyanate (FITC) (Santa Cruz 1:300). After washing in PBS samples were observed and captured using a Leica DM 2500 fluorescence microscope equipped with a DFC7000 camera or a Nikon A1 Rsi microscope using the software NisElements and Fiji software to process images.

4.2.5 Osteoblast proliferation and differentiation

To study the effect of LPA and 1,25D3 on hOB proliferation and differentiation the same culture 3D model described for collagen contraction was used.

Proliferation was tested using ATP quantification Kit (ViaLight Cambrex). At time 0 and after 1, 3, 6 and 12 days of culture of hOBs in collagen gel enriched with 1,25D3 10^{-7}M, LPA 1 μM or the combination of both, cells were lysed with cell lysis reagent and treated with ATP monitoring reagent that utilizes luciferase which catalyses the formation of light from ATP and luciferin. Light produced, that was linearly related to the intracellular ATP concentration, was measured by a luminometer and expressed as relative luminescence units (RLUs). Data were reported as mean ± SD of three experiments for each stimulus from each time point and were expressed as percentage compared to the control.

Alkaline phosphatase activity (APA), was determined by an assay based on the hydrolysis of p-nitrophenylphosphate to p-nitrophenol. hOB in the collagen gel containing either 1,25D3 (100 nM) or LPA (1 μM) or the combination of both after 1, 3 and 6 days of culture gels containing cells were rinsed and homogenized on ice for 2 x 10 sec using a Branson 250 sonifier

(Branson Ultrasonics, Danbury, USA) in 100 μl PBS. To 50 μl of this solution were added 50 μl of substrate (1mM paranitrophenyl-phosphate in 1 M diethanolamine + 1 mM $MgCl_2$ pH 9.8). The mixture was incubated at 37°C until the colour was comparable with a standardized series of paranitrophenol and measured in a micro plate spectrophotometer at 410 nm (Bio-Rad, Milan, Italy).

For mineralization studies, after 3 weeks of culture renewing the stimulus every 3 days in FAFA-IMDM containing 10 mM β-glycerophosphate and 50 μg/ml L-ascorbic acid, the 1,25D3 collagen cultures were treated overnight with 5 μg/ml calcein. After washing with PBS, mineralized nodules were acquired using a BP 515-560 excitation filter and a Leica DFC7000 camera. Three random calcein fluorescence images in fields of 1.0912 μm^2 were analyzed using Qwin Image Analysis software (Leica) in each experiment that was repeated 4 times (n=12).

4.2.6 Migration test

The effect of LPA, 1,25 D3 or LPA+1,25 D3 on cell migration was investigated in the 3D collagen medicated scaffold with the tested factors at the following concentrations: 1,25D3 100 nM; LPA 2,5 μM. Cells were seeded on a 24-well non-adhesive plate at 1 x 10^6 cells/well and then the collagen scaffolds with or without LPA, 1,25D3 or both were placed in the plate and incubated at 37°C in gentle soaking. After 8 days, the samples were washed with PBS and some samples stained with phalloidin-DAPI for confocal observations.

4.2.7 *In vitro* culture model of bone fracture

Trabecular vital bone fragments in FAFA-IMDM without serum were mixed at a ratio 1:1 in the collagen solution prior to gel formation together or without the factor to be tested (1,25D3

10^{-7}M; LPA 1 μM) or the combination of both and compared after 3 weeks of culture in calcification medium described in calcein staining paragraph. After the culture period, the specimens were fixed at 4°C for 2 days in 4% phosphate-buffered formaldehyde and dehydrated in ascending ethanol for one night prior to three-step impregnation in a methylmethacrylate (MMA) for at least three days. For embedding, specimen blocks were impregnated in 80% (vol/vol) stabilized MMA, 20% (vol/vol) Plastoid N (Rohm Pharma, Germany) for 2 h in uncapped vials under vacuum and imbedded in capped 10ml glass vials at 37°C overnight. After the polymerization, the glass vials were removed and moistened sections (100 μm) were cut on a Leica SP 1600 Saw Microtome with a rotating diamond saw blade for high-quality sample preparation of hard materials for microscopic analysis and mounted on polyethylene slides. The sections were stained using haematoxylin-eosin, light-green and fucsin acid solution for histological evaluation.

4.2.8 Mechanical properties

Tensile strength of samples was measured with Instron 5564 testing instrument (Instron Corporation, Canton, MA). The device comprises an electronic control console, a loading frame capable of testing up to 2.5 N in tension, and a drive system that induces tension on the samples until rupture. The test was conducted with a constant elongation speed of 0,05 mm/sec. The machine conveyed real-time displacement of the load frame and strength employed on the sample; strength at the breaking point was used as parameter to compare the new formed tissue in the collagen medicated matrix between the bone fragments. All samples were tested in triplicate and data are presented as mean ± standard deviation (DS).

4.2.9 *In vivo* experiments

In vivo experiments were performed in collaboration with Faculté de Médecine INSERM UMR 957_LPRO (Nantes, France), on 8-week-old nude mice. We carried out a hole of 1 mm in diameter at the level of the proximal epiphysis of the right tibia; this hole does not cross the two sides of bone but only one cortical. The hole has been performed with an instrument for dental use composed of a drill with adjustable speed and a tip with a diameter of 1mm. To test whether collagen may lead to an improvement in the repair of the damage, the mice were initially divided into 4 groups, each consisting of 3 mice: a negative control group, a group that was injected with collagen, a group that was injected with collagen + LPA (1μM) and a group to which was injected collagen with cells. Collagen has a concentration of 2 mg / ml and the cells were added at a concentration of 1.5 x105 in 25μl. In order to administer the cells *in vivo* is necessary that they are not suspended in the culture medium, because this could induce sensitization or immune reactions in animals so after counting the cells are centrifuged again and re-suspended in PBS before mixing them in a 1:1 ratio to collagen (collagen 12μl and 12μl PBS + cells). For the animal group to which was injected only collagen or collagen + LPA, similarly it was prepared in a mixture 1:1 with PBS. Before surgery, it was made an intraperitoneal injection with a solution composed of 165μl of 50mg/ml Ketamine (Imagene 500), 200μl of Xylazine (Rompun 2%) and just enough sterile water to 1ml; shortly after it was given morphine for pain relief, and a second dose of morphine was administered the day after. The animals were sacrificed after 7 days and from each was taken the right leg (the one in which it was made the hole) and from three animals sample was also taken the left leg as a control. The samples were subjected to analysis with μ-CT.

All procedures involving mice were conducted in accordance with the institutional guidelines of the French Ethical Committee (CEEA. PdL.06).

4.2.10 µ-CT

An X-ray computerized microtomography (micro Computerized Tomography abbreviated µ-CT) is a miniaturized form of the traditional Tomography Computerized Axial (TAC). As the letter than, it will allow to reconstruct the internal structure of opaque bodies without destroying them and this aspect is a great advantage compared to conventional microscopy techniques that provides information on the structure inside the sample considered only if the sample is treated and sectioned (74).

The µ-CT uses of an X-ray tube, X-ray generator, and a radiator detector. The X-ray source emits a thin collimated beam of radiation, in order to affect only a narrow section of the sample, the beam invests the sample and interacts with the matter being so attenuated by that, in a way strictly dependent of its internal composition. The radiation that emerges from the sample hits a radiation detector of the type CCD (Charge Coupled Device) that, once collected data, transfers them to a suitable computer. The CCD sensor, charge-coupled sensor surface was the first detector to be marketed with the beginning of the digital age. It is composed of three parts:

- the phosphor screen, which converts X-rays into visible light;
- a support conduction in the optical fiber, which conducts the radiation visible to the CCD chip, screen unit containing diodes and capacitors;
- The CCD chip which detects the luminous radiation and converts it into an electrical signal.

Once the X-rays strike the phosphor screen are transformed into light radiation. The latter than hits the photodiode in the CCD chip. At this point the diodes become conductive and the current

flowing through them goes to download the capacitors directly connected to them, which will have an instantaneous voltage across them inversely proportional to the photon flux. In this sister each diode represents a pixel.

When the integration period of the detector has been terminated, a series of switches are closed and then the discharge of each capacitor is transferred to a recording system of this data that is composed by other capacitors. Thereafter, the charge present on the capacitors of the register is transmitted to an analog-digital converter that transmits the data to the processing system. After that this transfer took place, the switches are reopened and the capacitors connected to the photodiodes are reloaded. At this point can be a new period of integration. The characteristics of this detector are: 1) ability to detect radiation also for long exposures without problems of non linearity and thermal saturation; 2) low background noise.

This allows generating 3D images with a high signal/noise ratio (SNR) and with high spatial resolution. This characteristics for conventional CT-scanners is 1/2,5 mm which corresponds in term of voxels (volume elementary body) to 1/10 mm^3.

We used high-resolution X-ray micro-CT system for small-animal imaging SkyScan-1076 (SkyScan, Kartuizersweg, Belgium) with these parameters: pixel size 9 μm, 50kV, 0.5-mm Al filter and 0.7 degree of rotation step. Reconstructed axial, sagittal and coronal images were taken using Micro-CT viewer program: Dataviewer. Three-dimensional reconstructions and analysis of bone parameters were performed using CTvox and CTan software (SkyScan).

4.2.11 Statistical Analysis

Means of groups were compared by analysis of variance and Bonferroni Student's two tailed t test was applied to evaluate differences in cell motility, proliferation, APA, cell mineralization,

collagen contraction and mechanical properties. The conventional $p \leq 0.05$ level was considered to reflect statistical significance.

4.3 Results and Discussion

4.3.1 Collagen characterization

The collagen was characterized by silver staining (Figure 16). The samples were compared with a standard commercial collagen I at a concentration of 2mg/ml and they were loaded 10 µl = 20 µg (Coll I from human placenta, Sigma). It was compared to the collagen extracted from rat tails and the collagen produced by osteoblasts in culture. As can be seen from the figure the collagen standard presents a doublet both high molecular weight and there is also one more evident at lower molecular weight. The collagen extracted from rat tails (lane 1) has a track similar to that of the standard, however with the bands more evident, probably due to a greater protein concentration. The collagen produced by osteoblasts in culture instead (lane 2) has a more dirty track and the separation of proteins is not obvious. From quantification with BCA emerges that the collagen from rat tails has a concentration of 3.5 mg/ml while for the collagen by osteoblasts concentration is only 0.3 mg/ml (Table 1).

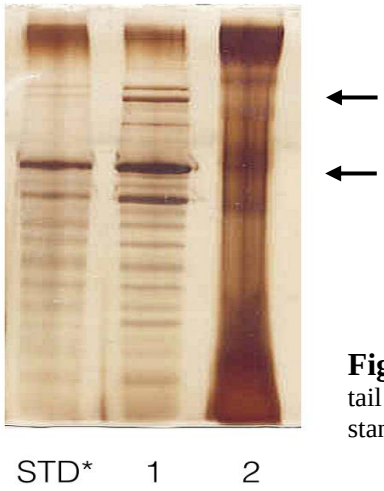

Fig. 16: Silver staining of collagen. Lane 1 collagen extracted from rat tail tendons, lane 2 collagen produced by osteoblast in culture. STD* is a standard of collagen I from human placenta purchased by Sigma.

	Rat tail	hOB
% collagen Sirius Red/BCA	95%	5%
mg/ml collagen	3.5	0.3
pH	2.3	7.3

Table 1: Quantification of collagen in mg/ml and purity percentage of the two samples tested.

The collagen is caused to precipitate and aggregate into native bundles by raising the ionic strength an pH to physiological levels. The collagen extracted from tendons was mixed with culture medium and with NaOH to bring the pH to 7.6. The solution was displayed at different intervals of time with the electron microscope in order to evaluate the assembly and the precipitation of collagen.

In figure 17 there is a progressive precipitation of collagen at different time intervals and after 24 hours there is the formation of the aligned collagen bundles. The surface of collagen gel show mats of long bundles usually straight and often branching, occasionally with a helical twist. It is usual also to observe the larger bundles in a single field roughly oriented in the same direction. Collagen can be employed to provide a two-dimensional substratum with cells seeded on the surface (Figure 18A) or a three-dimensional substratum incorporating cells prepared by mixing cells and collagen before seeding in the plate (Figure 18B).

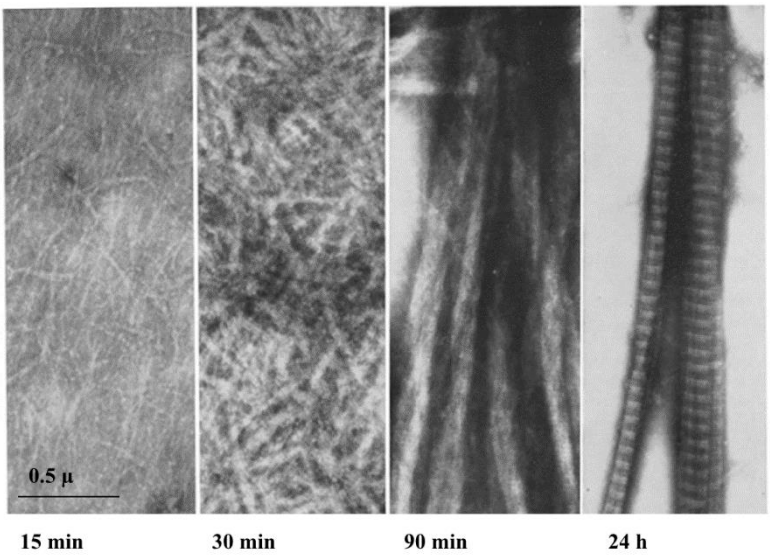

Figure 17: Stages in the assembly of collagen bundles. Cuvette sampled at 15, 30, 90 min and after 24 h. In the first and second picture we can see small disordered collagen fibers, the third image shows the beginning of the assembly of the fibers and, finally, after 24 hours we can see the final form of the collagen bundles.

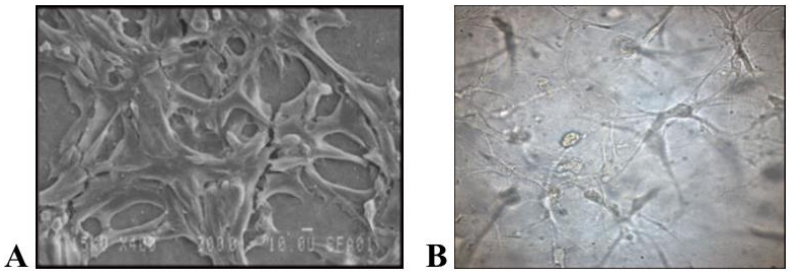

Figure 18: Osteoblast growing on collagen substrate (A) and osteoblast growing in a 3D matrix of collagen (B).

4.3.2 Gel contraction

Putting bone fragments within a collagen gel with HOB in 3D culture we have seen the approach of these fragments, and then the contraction of the gel that after 3 weeks form a real three-dimensional structure that includes the bone fragments (Figure 19). To test whether the contraction is due to the presence of cells or is an intrinsic property of the collagen we compared two types of gels: one with osteoblasts and one without osteoblasts. The bone fragments were inserted to check the contraction of the gel. Comparing these first two models is evident that the

gel contraction is cell mediated (Figure 20A), indeed there is no bone fragment approach if hOB were not present (Figure 20B).

Were subsequently made tests with cells at different concentrations within the collagen gel and it was observed that the time required for the approach of the fragments is concentration-dependent, in fact the higher was the concentration of osteoblasts in the gel, less was the time required to obtain the complete approach of the bone fragments (Figure 21).

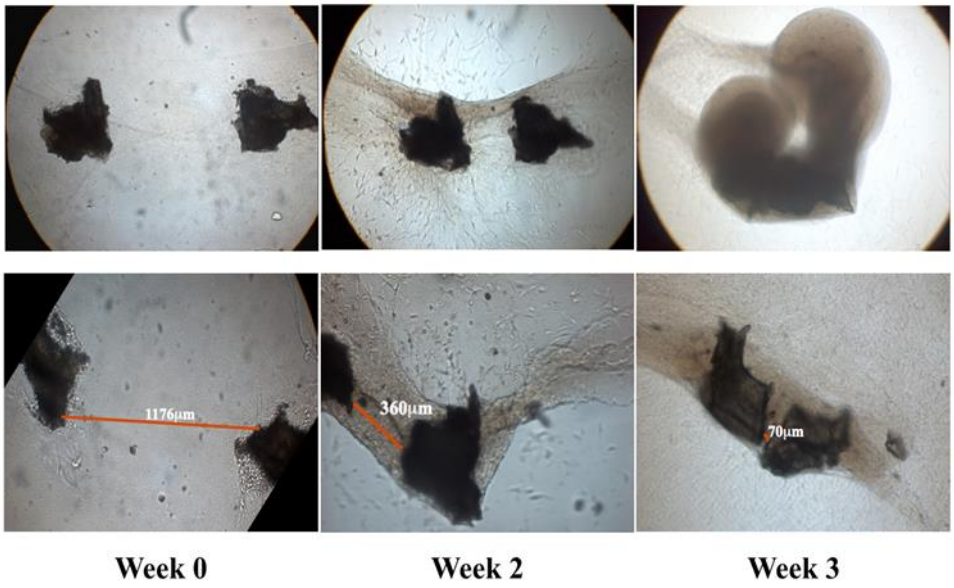

Figure 19: Approach of two bone fragments inside the collagen gel and the formation, after 3 weeks, of a structure that include the bone fragments.

When cells were added to the gel at a concentration of 100 cells/ml no contraction was seen at all the incubation time studied, also at the concentration of 1000 cells/ml was seen few gel contraction and only at the longer time of cell culture (24 and 48 days). Only at concentration higher than $1x10^4$ cells/ml we obtained a complete approach of the fragments but if at 10^4 cells/ml it was obtained in 24 days of culture, with 10^5 cells/ml and 10^6 cells/ml it was obtained in 12 days, whereas with a cell number of 10^7 cells/ml in the gel total approach of the fragments was obtained just after 6 days of culture.

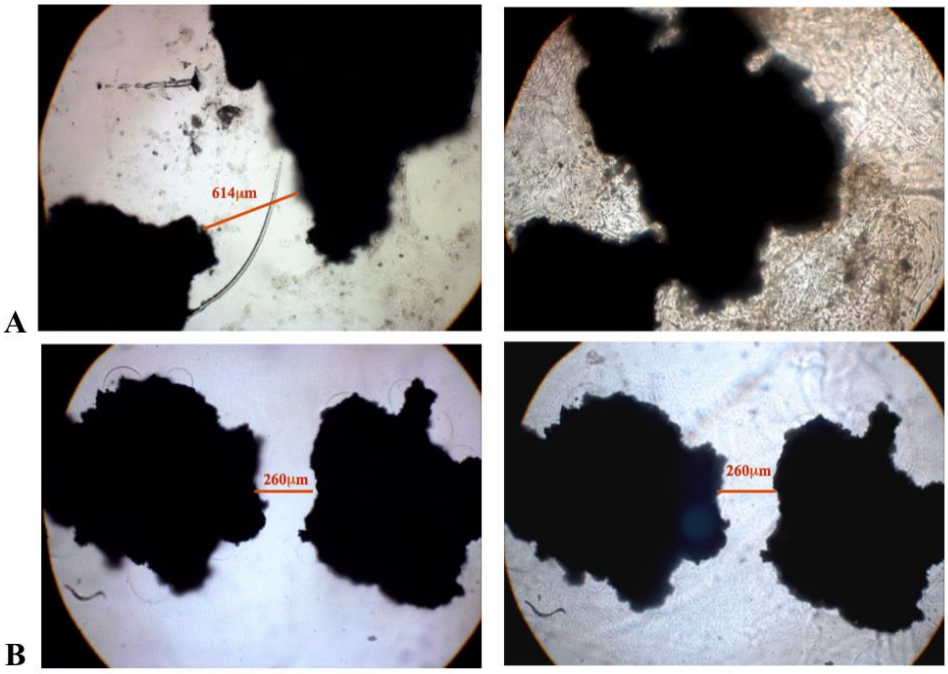

Figure 20: Approach of two bone fragments inside the collagen gel in the presence of hOB (A). No approach if osteoblast are not inoculated in the gel (B).

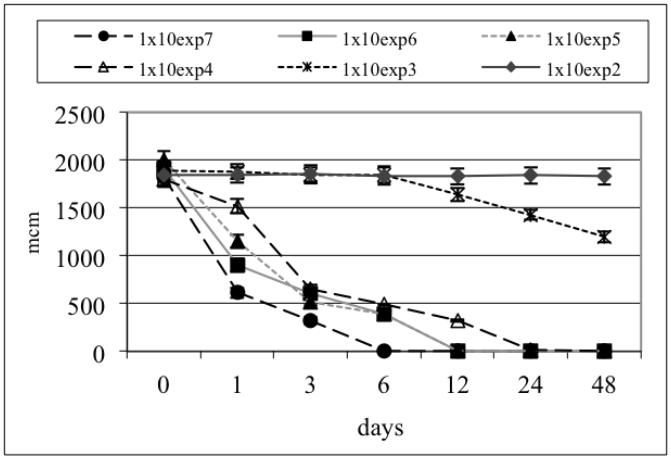

Figure 21: The time required for the total approach is lower if the concentration of cells present within the collagen gel is higher. If the concentration of cells is equal to $1x10^2$ or $1x10^3$ we do not have the approach of the fragments even after 48 days of culture.

These results are comparable with those reported in a previous study in which MG-63 cells were used in a collagen gel and where it was evaluated in the contraction of the gel the involvement

of the cytoskeleton. When cells were treated with Cytochalasin D, an actin depolymerizing agent, it was seen that the contraction was inhibited (125).

It has been hypothesized that the mechanism involved in this contraction is related to the activity of the proteine Rho-kinase because ROCK is an effector of Rho and functions by inhibiting myosin light-chain phosphatase (100), this inhibition results in an accumulation of phosphorylated myosin light chain kinase and the development of myosin filaments that interact with actin filaments and form highly contractile stress fibers. In addition, Rho kinase regulates cofilin phosphorylation through activation of LIM-kinase (130). Cofilin phosphorylation inhibits actin depolymerization and promotes reorganization of the actin cytoskeleton to develop stress fibers.

It was also demonstrated that, in contrast to smooth muscle cells, in which the level of intracellular Ca^{2+} is the dominant system regulating contraction, in fibroblasts and osteoblasts increasing of intracellular Ca^{2+} is not sufficient to promote contraction. These cells contraction requires activation of small GTPase Rho and the associated Rho Kinase (131).

So we compared osteoblasts' mediated contraction under the stimulation of a Rho-kinase antagonist (Y-27632), an agonist of Rho-kinase (LPA) and an inhibitor of microtubule formation (Nocodazole).

The stimuli were added both within the gel (in the mixture of collagen and cells), either in culture medium added after 24 hours incubation time at 37°C.

We saw that, at the same cell concentration in the gel, with the stimulation of LPA there is an increase in the contraction of the collagen compared to the control, while the contraction is decreased in the presence of both the Rho-kinase inhibitory factor and nocodazole. In fact as we can see in figure 22, by placing the control as 0% contraction is possible to note that Y-27632 causes a relaxation of the collagen matrix (-34,6 %) compared to the control, while the activator

of Rho-kinase pathway, LPA, promotes the contraction of the gel (+23,3 %) compared to the control. The nocodazolo destroys the microtubules, part of the cellular cytoskeleton, and therefore it does not allow the contraction of the gel, which then relaxes (-85,6 %). Our results are consistent with prior studies obtained with fibroblast (132) and show that treatment of hOB cells embedded in collagen gels with Y-27632 resulted in a inhibition of contraction.

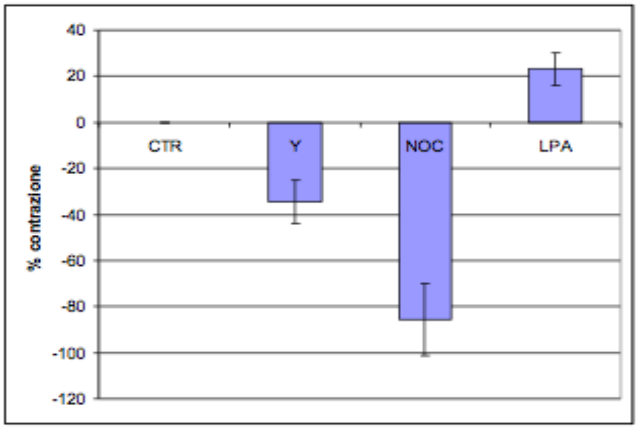

Figure 22: Schematic representation of collagen contraction mediated by LPA and instead the relaxation of the matrix caused by Y-27632 and by NOC. Contraction is expressed as a percentage, compared to the control that is considered as 0%.

4.3.3 Human osteoblasts evidenced a Rho mediated actin cytoskeleton modifications

Figure 23 shows representative images of human primary osteoblasts visualized by phalloidin staining for actin when cultured in collagen-coated coverslips (A-C) and in collagen 3D matrices (D-F). Cells in monolayer were well spread with lamellipodia and actin stress fibers (A) with more compact cell morphology and greater density of stress fibers when the Rho-kinase agonist (LPA 2,5 μM) was added (B) whereas when Rho-kinase antagonist (Y-27632) was added to culture media, cells appeared with stellate-like shape and cytoplasmic projections and actin-

containing ruffles only along the cell margins (C). A markedly different appearance was seen when human osteoblasts were embedded in 3D collagen matrices where osteoblasts projected a dendritic network of extensions (D) that retract when LPA was added to the gel (E) while the Rho-kinase antagonist addition to the gel caused an overall increase in size and branching of the dendritic network (F). Our findings indicated that human primary osteoblasts in 3D floating collagen matrices developed neuronal-like dendritic morphology distinct from osteoblasts on coverslips and responded differently to LPA by withdrawal their extensions rather than increasing stress fibers. Actin localized cortically and concentrated at the tips of cell extensions in control and Y treated gels or in ruffles and at the tips of cell extensions in LPA treated cells. The cytoskeletal changes shown in LPA enriched gel could explain the gel contraction results shown in Figure 20 through by inhibition of cell protrusion and stimulation of cell contraction.

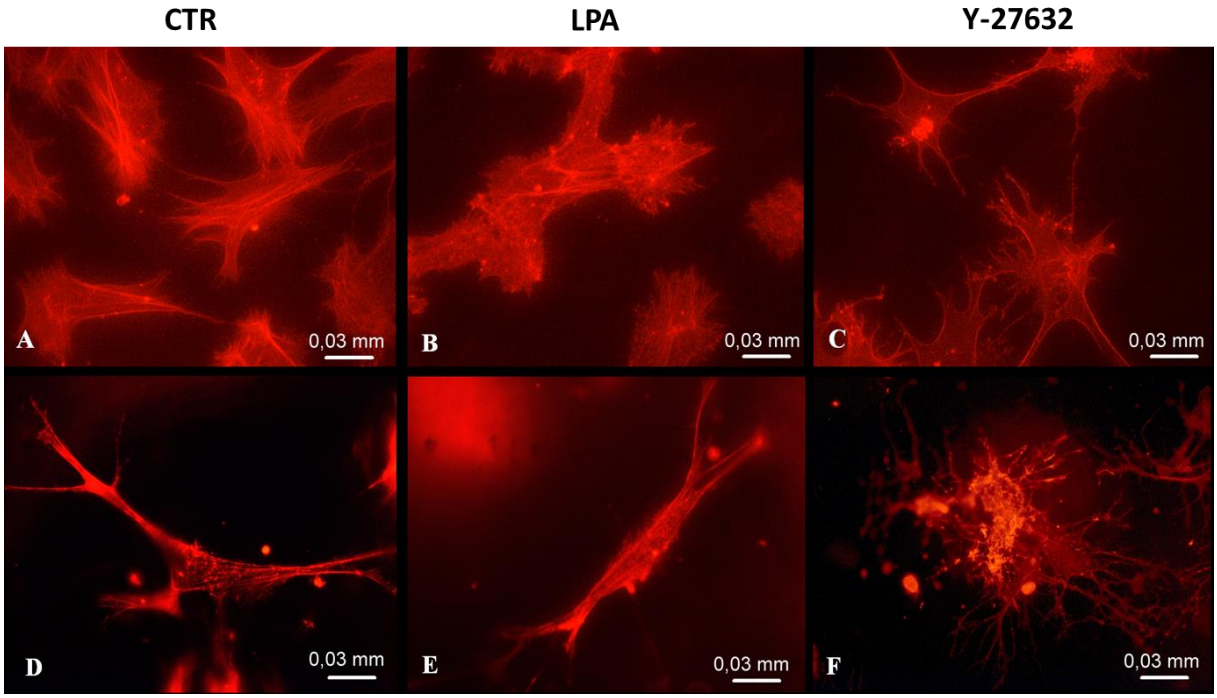

Figure 23: Fluorescence images of osteoblast in monolayer (A-C) and in collagen 3D matrix (D-F). Control osteoblast (A,D), osteoblast treated with LPA (B,E) and osteoblast treated with Y-27632 (C,F).

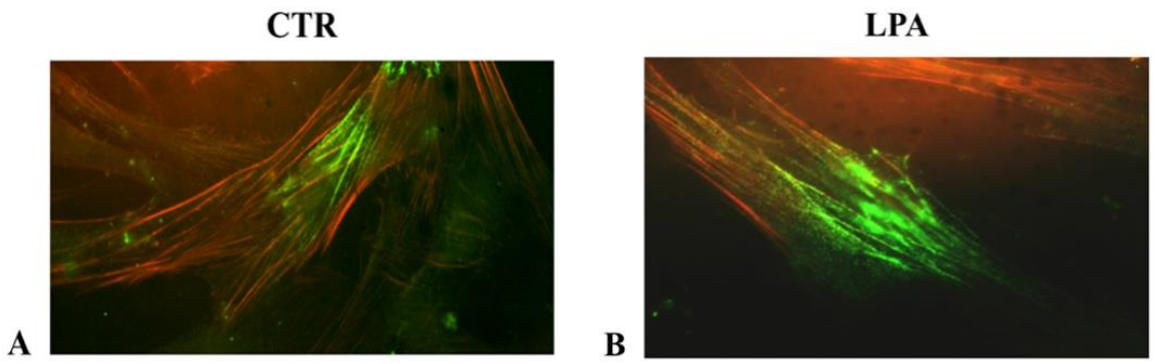

Figure 24: Primary human osteoblasts in fluorescence with actin filaments labeled with phalloidin (red) and myosin labeled with MLC fluorescent antibody (green). In the figure there are both control cells (A) and cells treated with LPA (B).

4.3.4 Human osteoblasts proliferation and differentiation in response to LPA

To understand if LPA added to collagen could be considered osteoconductive and not only mechanically active working in cytoskeleton reorganization in bone repair, we tested its activity on proliferation and differentiation of human primary osteoblasts when used alone or in combination with Vitamine D3 found in a recent publication to be a differentiating stimulus on osteoblasts (124). At the meantime we have tested if Vit. D3 enrichment in some extent could interfere with gel contraction.

Data confirmed an inhibition of proliferation of human primary osteoblast-like cells treated with D3 while LPA produced a significant increase in proliferation of primary cultures of human osteoblasts at the longer incubation times (6 and 12 days) as shown in Figure 24A. When LPA was added in combination with D3 the proliferative response of the cells was inhibited.

Stimulation of hOB with D3 (100 nM) or LPA (10 μM) led to increases in ALP activity at 1 day of cell incubation showing no more increased activity at longer incubation times. The co-

stimulation with both factors led to synergistic increase in ALP activity time-dependent (Figure 24B) together with an increased matrix mineralization (Figure 24C).

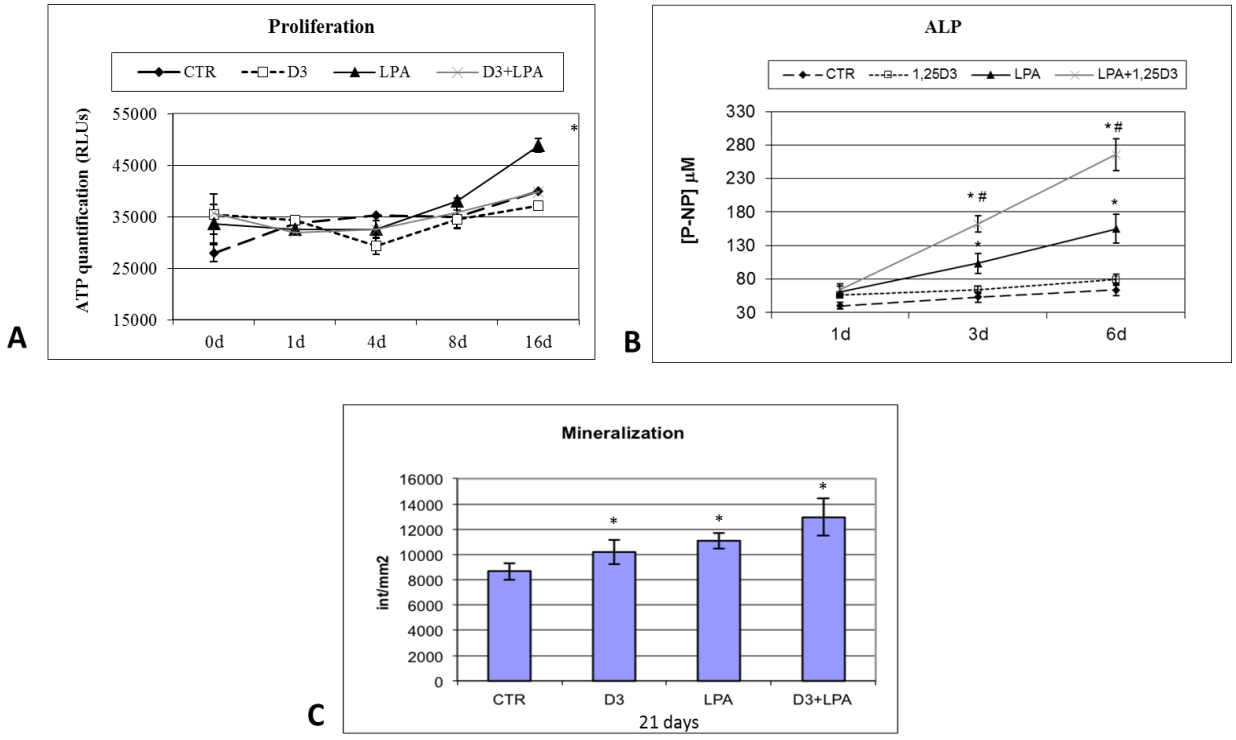

Figure 24: Human osteoblasts proliferation and differentiation in response to LPA used alone or in combination with Vitamin D3. LPA promotes human osteoblast proliferation, instead with the addition of VitD3 the proliferation decreases (A). The differentiation of osteoblasts is greater if we use the combination of LPA and VitD3 as stimulus, while LPA alone and VitD3 alone give meaningful results only in the short term (B). The mineralization of the extracellular matrix is favored by the stimulation with LPA and VitD3 in combination (C).

4.3.5 Human osteoblasts migration in response to LPA

We have evaluated the migration of cells within the gel with LPA after 8 days of culture. As we can see from the pictures (Figure 25), in the control gel, cells are present in greater quantities along the edge (A), but in the central part are less (B). Instead, the gel enriched with LPA is not only able to induce the migration of the cells in the inner part of the gel, but it seems also to regulate the orientation of the cells migrated in the gel.

With the confocal microscope were taken about 50 serial images at a distance of 2 μm from each other, so in total we were able to obtain images in a thickness of 100 μm. The presence of cells even at 100 μm from the edge of the gel indicates that the cells are migrated inside the 3D structure. It was not possible to evaluate the entire thickness of the gel as it is a few millimeters and the power of laser of the microscope is not so high as to be able to pass through it completely.

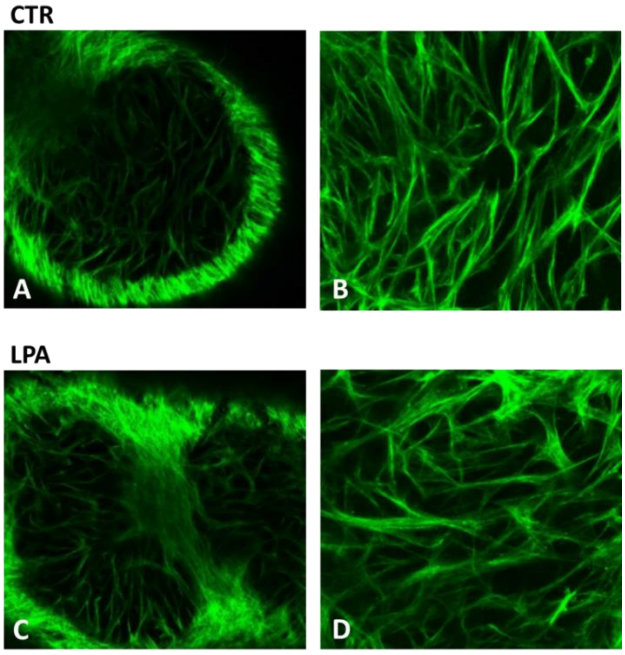

Figure 25: Confocal microscope images acquired at a distance of 2 μm from the others. Each images is the result of the union of 10 images. We can see the control gel (A-B) and the gel treated with LPA (C-D). These images were acquired with a 20x oil objective with a digital zoom 1x (A-C), zoom 2.2x (B-D).

4.3.6 LPA and D3 co-operate to expedite bone regeneration

A time-course approach study of bone fragments in the gel enriching the 3D collagen with LPA, 1,25D3 or LPA+1,25D3 showed that compared to the control, 1,25D3 does not speed up the approach of the bone fragments. According to (125) 1,25D3 treatment did not affect collagen gel contraction.

LPA or LPA+VitD3 increases the speed of contraction in the short-term (after 1, 3 and 6 days) and also provides to reach the total approach in 12 days instead of the 24 days required with VitD3 (Figure 26).

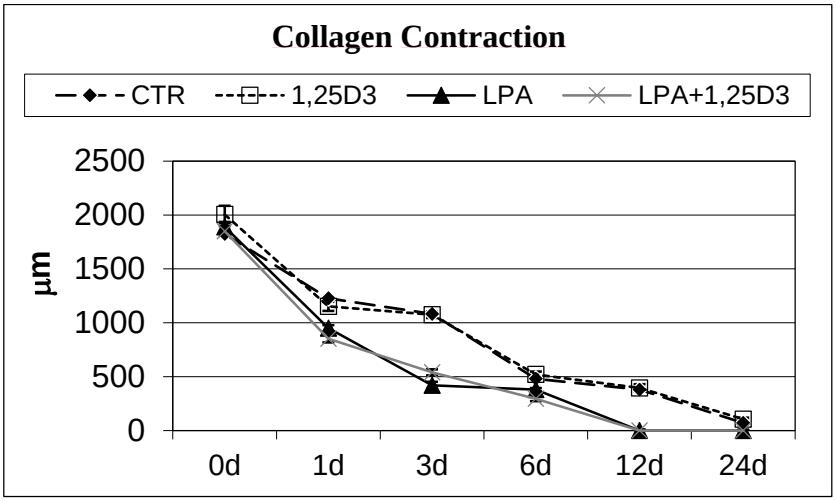

Figure 26: Contraction mediated by LPA or LPA+D3 allows complete approach of the fragments already after 12 days while in the gel with D3 alone we have complete approach only after 24 days.

The results of histology (Figure 27) of the new formed tissue around bone fragments shows the formation of a fibrous bone tissue within 3 weeks of culture. The addition of 1,25D3 to collagen at concentration of 0,1 mg/mL promotes the mineralization of the new formed tissue that shows also increased tensile strength (Figure 28).

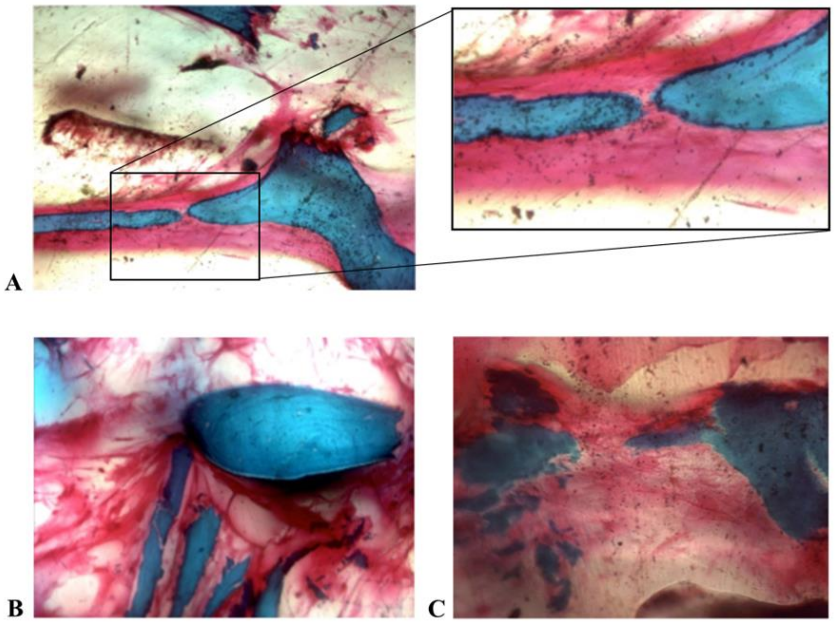

Figure 27: Histological images of collagen gel with bone fragments within. Staining with light green and fuchsin shows that there is the newly formed tissue between the fragments, but it is not mineralized yet.

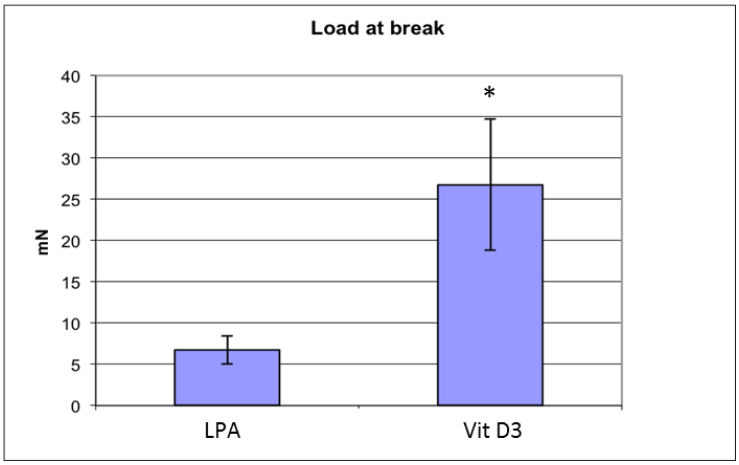

Figure 28: Load at break measured with the Instron instrument. The use of VitD3 increases the mechanical resistance to the traction of the collagen gel, compared to the gel treated with LPA.

4.3.7 *In vivo* experiment

Regarding the results obtained from *in vivo* test, three-dimensional images of the tibia were taken in four different conditions of treatment and then they were analysed (Figure 29).

It was also evaluated the bone density present inside the hole using the same diameter of the area of assessment and the same depth (1000 μm). The values obtained show that the percentage of bone volume compared to the total volume is greater in the sample in which the collagen was injected with cells or LPA compared to the control, and to the sample in which only the collagen was used to fill the hole (Figure 30). These are preliminary data to evaluate the difference between these conditions, and we will do further experiments with a larger number of animals for a statistical evaluation of the data. Moreover we will test LPA loaded gel together with D3 addition. We are also preparing samples for histological and immunohistochemical analysis on decalcified new formed tissue to evaluate the mineralization, inflammation and vascularization present in the callus and the repair of the damage.

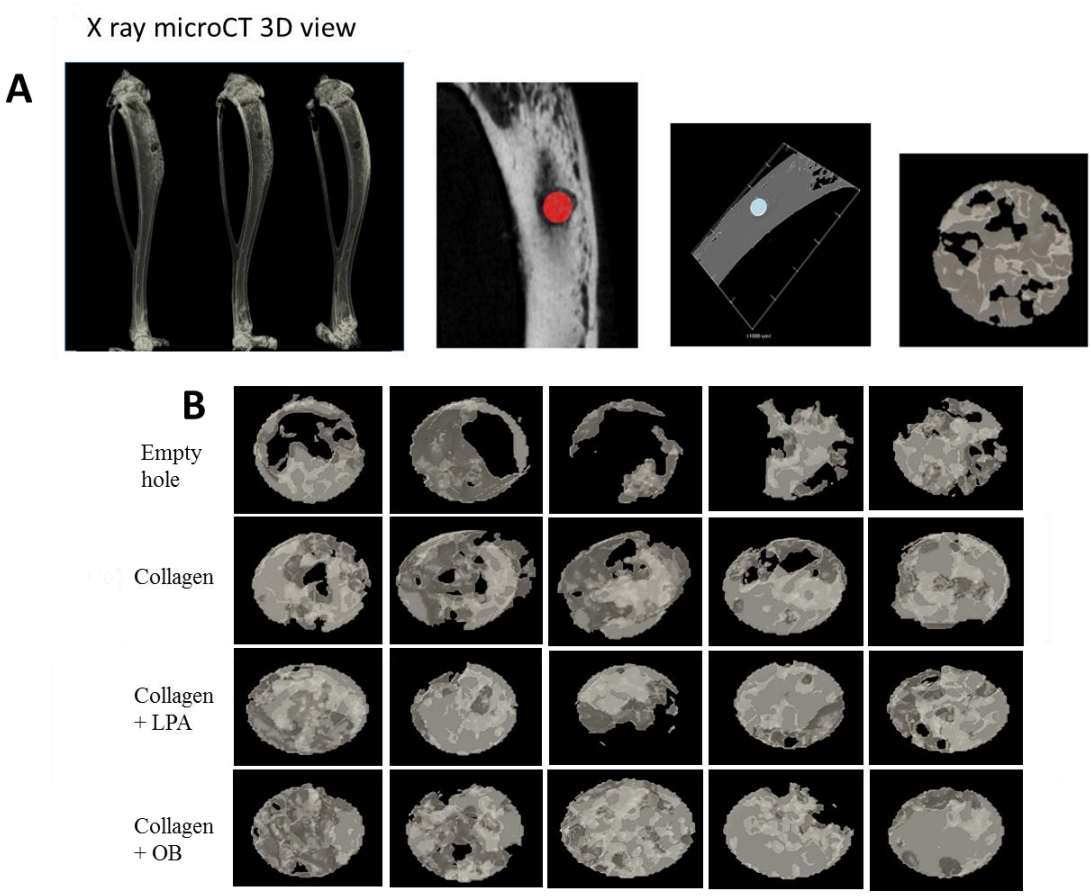

Figure 29: In the figure A we can see the position of the hole at the level of the proximal epiphysis of the tibia and the graphical display of the bone volume in relation to the total volume. In the figure B we can see the section considered and we can see the density of the bone volume. It can be seen as the bone volume is greater in the collagen+LPA and collagen+OB compared to the other two samples.

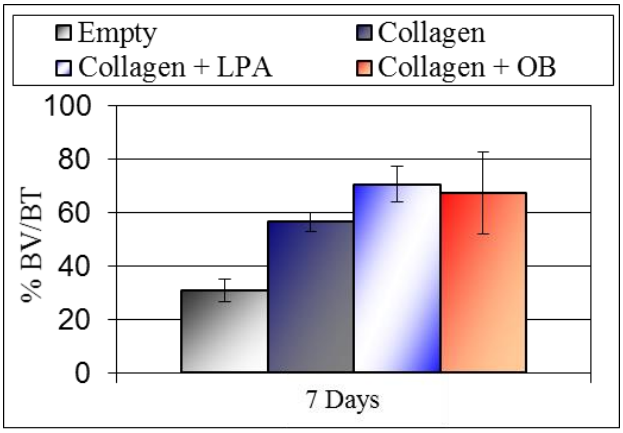

Figure 30: The bone volume was quantified in per cent after 7 days from the surgery, with the following formula: BV/TV where BV is bone volume and TV is the total volume.

4.4 Conclusions

Tissue regeneration by endogenous cells supplied from the defect area, without the necessity of cell transplantation, is a promising strategy in various fields of regenerative medicine. With regard to the bone, the defect regeneration by cell homing without cell transplantation is a rising approach lacking experimental testing. The migration of cells from the side of defect could be important to faster bone healing and speed bone regeneration thus the choices of an appropriate scaffold, which can facilitate cell migration increasing cellular infiltration, is of great importance.

In order to develop an injectable medicated scaffold which speeds bone formation in sinus lift augmentation, in bony void and in fracture repair, we have developed a medicated scaffold that: 1) promotes the repopulation by osteoblasts coming from the bone fragments adjacent to the damage; 2) is osteogenic; 3) favors the approach of bone fragments taking advantage of the contraction capacity of osteoblasts.

While the knowledge of the mechanisms that regulate the contraction of fibroblasts in wound healing are well known, the function and the ability of osteoblasts to contract the extracellular matrix are still unclear, although it has been hypothesized that the contraction capacity of osteoblasts may play an important role in forming bridges between fragments of fractured bone (117) or imparting an architecture during bone remodelling (126). Exploiting RhoA and ROCK-mediated cytoskeletal organization and actin-myosin-mediated cytoskeletal tension, we have obtained trough cell contraction a three-dimensional collagen matrix that reduces the distance between bone fragments. We have demonstrated that human primary osteoblasts, in a manner similar to fibroblasts, cultured in a 3D collagen matrix showed a global matrix remodelling that resulted in collagen contraction. Also, this contraction was Rho dependent. From these

preliminary data is our idea to add a Rho activator, LPA, to a collagen gel to be used as an active scaffold that, with its cell-mediated contraction, favors the closure of the gap between bone fragments. We have chosen LPA for different reasons; first of all its receptors couple to Rho and Rac to elicit changes in cytoskeletal organization (116), thereby regulating cell migration, chemotaxis and growth of a lot of cells and of osteoblasts through interactions with the LPA1 receptor. A second reason is that LPA is supposed to be a factor involved in the regulation of osteogenesis and bone remodeling, inducing *in vitro* osteoblasts' synthesis of some osteoinductive cytokines (127, 128) and committing mesenchymal stem cells to osteoblasts by stimulating their proliferation and inducing their differentiation (112). Third, recent *in vitro* and *in vivo* studies have shown that LPA, present at elevated levels at sites of tissue injury and inflammation as product of activated platelets (107), is also produced by bone cells and have identified its direct effect on various cellular activities that could mean control of bone mass and/or composition (108, 112).

LPA, together with EGF and TGFβ, are the only three growth factors known to synergistically co-operate with 1,25D3 in promoting hOB maturation. So, the combination of LPA with 1,25D3 in a controlled release format or as a coatings for metal and ceramic devices could have great potentials in a bone regenerative context like fracture non-unions and bone biomaterial integration.

Active vitamin D3 metabolites have direct effects on human osteoblast function and matrix calcification, providing mechanically robust mineralized bone collagen matrix as vitamin D receptor (VDR)-mediated events. Recently, we have shown that the loading of 1,25(OH)2D3 positively influences the late events in osteoblast maturation and the induction of osteogenic markers so, accordingly to other studies, we found a positive effect on *in vitro* osteogenesis using calcitriol within a 3D scaffold (129). Of additional significance are studies reporting cross-

talk between 1,25D3 and growth factors known to be active on hOB growth, matrix synthesis and mineralization e.g. TGFβ, EGF, PTH, Wnt signalling ligands and LPA.

In conclusions, in order to develop an injectable enriched scaffold which speeds bone formation in fracture repair, we have demonstrate that:

- collagen is an excellent substrate for human primary osteoblasts.
- the mechanism involved in cell contraction is mediated by Rho-kinase protein, but it is still unclear which protein downstream of the Rho cascade is responsible for the cytoskeletal rearrangement.
- LPA alone or in combination with VitD3 may be useful to functionalize the collagen scaffolds like has been done in recent published works using growth factors.

For these reasons, we think that an injectable scaffold enriched with LPA and Vitamin D3 could be used *in vivo* to accelerate bone growth and fracture healing acting as a substrate that cells from the damaged tissue can attach to and populate.

5. References

1. Archer, C. W.; McDowell, J.; Bayliss, M. T.; Stephens, M. D.; Bentley, G. Phenotypic modulation in sub-populations of human articular chondrocytes *in vitro*. J. Cell Sci. 97:361-371; 1997.
2. Baer, P. C.; Geiger; H. Adipose-derived mesenchymal stromal/stem cells: tissue localization, characterization, and heterogeneity. Stem Cells Int. 2012:812693; 2012.
3. Bendinelli, P.; Matteucci, E.; Dogliotti, G.; Corsi, M. M.; Banfi, G.; Maroni, P.; Desiderio, M. A. Molecular basis of anti-inflammatory action of platelet-rich plasma on human chondrocytes: mechanisms of NF-kB inhibition via HGF. J. Cell. Physiol. 225(3):757-766; 2010.
4. Bianchi, F.; Maioli, M.; Leonardi, E.; Olivi, E.; Pasquinelli, G.; Valente, S.; Mendez, A. J.; Ricordi, C.; Raffaini, M.; Tremolada, C.; Ventura, C. A new non-enzymatic method and device to obtain a fat tissue derivate highly enriched in pericyte-like elements by mild mechanical forces from human lipoaspirates. Cell Transplant. 22(11):2063-2077; 2013.
5. Black, L. L.; Gaynor, J.; Adams, C.; Dhupa, S.; Sams, A. E.; Taylor, R.; Harman, S.; Gingerich, D. A.; Harman, R. Effect of intrarticular injection of autologous adipose-derived mesenchymal stem and regenerative cells on clinical signs of chronic osteoarthritis of the elbow joint in dogs. Vet. Ther. 9(3):192-200; 2008.
6. Bosetti, M.; Boccafoschi, F.; Leigheb, M.; Bianchi, A. E.; Cannas, M. Chondrogenic induction of human mesenchymal stem cells using combined growth factors for cartilage tissue engineering. J. Tissue Eng. Regen. Med. 6:205-213; 2012.
7. Breyner, N. M.; Hell, R. C.; Carvalho, L. R.; Machado, C. B.; Peixoto, I. N.; Valerio, P.; Pereira, M. M.; Goes, A. M. Effect of a three-dimensional Chitosan porous scaffold on the

differentiation of mesenchymal stem cells into chondrocytes. Cells Tissues Organs 191(2):119-128; 2010.

8. Cox, W. G.; Singer, V. L. A high-resolution, fluorescence-based method for localization of endogenous alkaline phosphatase activity. J. Histochem. Cytochem. 47(11):1443-1456; 1999.
9. Crouch, S. P.; Kozlowski, R.; Slater, K. J.; Fletcher J. The use of ATP bioluminescence as a measure of cell proliferation and cytotoxicity. J. Immunol. Methods 160(1):81-88; 1993.
10. Elsdale, T.; Bard, J. Collagen substrata for studies on cell behaviour. J. Cell Biol. 54:626-637; 1972.
11. Emans, P. J.; Jansen, E. J.; van Iersel, D.; Welting, T. J.; Woodfield, T. B.; Bulstra, S. K.; Riesle, J.; van Rhijn, L. W.; Kuijer, R. Tissue-engineered constructs: the effect of scaffold architecture in osteochondral repair. J. Tissue Eng. Regen. Med. 7(9):751-756; 2013.
12. Farndale, R. W.; Sayers, C. A.; Barrett, A. J. A direct spectrophotometric microassay for sulphated glycosaminoglycans in cartilage cultures. Connect. Tissue Res. 9(4):247-248; 1982.
13. Follenzi, A.; Sabatino, G.; Lombardo, A.; Boccaccio, C.; Naldini, L. Efficient gene delivery and targeted expression to hepatocytes *in vivo* by improved lentiviral vectors. Hum. Gene Ther. 13:243–260; 2002.
14. Freyria, A. M.; Mallein-Gerin, F. Chondrocytes or adult stem cells for cartilage repair: the indisputable role of growth factors. Injury 43(3):259-265; 2012.
15. Grace, H. L.; LaValley, M.; McAlindon, T.; Felson, D. T. Intra-articular hyaluronic acid in treatment of knee osteoarthritis. J. A. M. A. 290(23):3115-3121; 2003.
16. Hale, L. V.; Ma, Y. F.; Santerre, R. F. Semi-quantitative fluorescence analysis of calcein binding as a measurement of *in vitro* mineralization. Calcif. Tissue Int. 67(1):80-84; 2000.

17. Hamid, A. A.; Idrus, R. B.; Saim, A. B.; Sathappan, S.; Chua, K. H. Characterization of human adipose-derived stem cells and expression of chondrogenic genes during induction of cartilage differentiation. Clinics 67(2):99-106; 2012.
18. Hunziker, E. B. Articular cartilage repair: basic science and clinical progress. A review of the current status and prospects. Osteoarthritis Cartilage 10:432-463; 2002.
19. Jurgens, W. J.; Kroeze, R. J.; Zandieh-Doulabi, B.; van Dijk, A.; Renders, G. A.; Smit, T. H.; van Milligen, F. J.; Ritt, M. J.; Helder, M. N. One-step surgical procedure for the treatment of osteochondral defects with adipose-derived stem cells in a caprine knee defect: a pilot study. Biores. Open Access 2(4):315-325; 2013.
20. Kastrinaki, M. C.; Andreakou, I.; Charbord, P.; Papadaki, H. A. Isolation of human bone marrow mesenchymal stem cells using different membrane markers: comparison of colony/cloning efficiency, differentiation potential, and molecular profile. Tissue Eng. Part C Methods 14:333-339; 2008.
21. Kershaw, E. E.; Flier, J. S. Adipose Tissue as an Endocrine Organ. J. Clin. Endocrinol. Metab. 89(6):2548-2556, 2004.
22. Kurita, M.; Matsumoto, D.; Shigeura, T.; Sato, K.; Gonda, K.; Harii, K.; Yoshimura, K. Influences of centrifugation on cells and tissues in liposuction aspirates: optimized centrifugation for lipotransfer and cell isolation. Plast. Reconstr. Surg. 121(3):1033-1041; 2008.
23. Kuroda, T.; Matsumoto, T.; Mifune, Y.; Fukui, T.; Kubo, S.; Matsushita, T.; Asahara, T.; Kurosaka, M; Kuroda, R. Therapeutic strategy of third-generation autologous chondrocyte implantation for osteoarthritis. Ups. J. Med. Sci. 116(2):107-114; 2011.

24. Leunig, M.; Tibor, L. M.; Naal, F. D.; Ganz, R.; Steinwachs, M. R. Surgical technique: second generation bone marrow stimulation via surgical dislocation to treat hip cartilage lesions. Clin. Orthop. Relat. Res. 470(12):3421-3431; 2012.
25. Mestak, O.; Sukop, A.; Hsueh, Y. S.; Molitor, M.; Mestak, J.; Matejovska, J.; Zarubova, L. Centrifugation versus PureGraft for fat grafting to the breast after breast-conserving therapy. World J. Surg. Oncol. 12:178; 2014.
26. Noël, D.; Caton, D.; Roche, S.; Bony, C.; Lehmann, S.; Casteilla, L.; Jorgensen, C.; Cousin, B. Cell specific differences between human adipose-derived and mesenchymal–stromal cells despite similar differentiation potentials. Exp. Cell Res. 314:1575-1584; 2008.
27. Pfaffl, M. W. A new mathematical model for relative quantification in real-time RT-PCR. Nucleic Acids Res. 29(9):2002-2007; 2001.
28. Sakaguchi, Y.; Sekiya, I.; Yagishita, K.; Muneta, T. Comparison of human stem cells derived from various mesenchymal tissues: superiority of synovium as a cell source. Arthritis Rheum. 52:2521-2529; 2005.
29. Samuels, J.; Kransnokutsky, S.; Abramson, S. B. Osteoarthritis: a tale of three tissues. Bull. NYU Hosp. Jt. Dis. 66(3):244-250; 2008.
30. Sharkey, P. F.; Cohen, S. B.; Leinberry, C. F.; Parvizi, J. Subchondral bone marrow lesions associated with knee osteoarthritis. Am. J. Orthop. 41(9):413-417; 2012.
31. Shenaq, D. S.; Rastegar, F.; Petkovic, D.; Zhang, B. Q.; He, B. C.; Chen, L.; Zuo, G. W.; Luo, Q.; Shi, Q.; Wagner, E. R.; Huang, E.; Gao, Y.; Gao, J. L.; Kim, S. H.; Yang, K.; Bi, Y.; Su, Y.; Zhu, G.; Luo, J.; Luo, X.; Qin, J.; Reid, R. R.; Luu, H. H.; Haydon, R. C.; He, T. C. Mesenchymal progenitor cells and their orthopaedic applications: forging a path towards clinical trials. Stem Cells Int. 16:519028; 2010.

32. Tullberg-Reinert, H.; Jundt, G. In situ measurement of collagen synthesis by human bone cells with a Sirius Red-based colorimetric microassay: effects of TGFβ2 and ascorbic acid. Histochem. Cell Biol. 112:271-276; 1999.
33. Veronesi, F.; Maglio, M.; Tschon, M.; Aldini, N. N.; Fini, M. Adipose-derived mesenchymal stem cells for cartilage tissue engineering: state-of-the-art in *in vivo* studies. J. Biomed. Mater. Res. A. 102(7):2448-2466; 2014.
34. Xue, J. X.; Gong, Y. Y.; Zhou, G. D.; Liu, W.; Cao, Y.; Zhang, W. J. Chondrogenic differentiation of bone marrow-derived mesenchymal stem cells induced by acellular cartilage sheets. Biomaterials 33:5832-5840; 2012.
35. Spector M. Novel cell-scaffold interactions encountered in tissue engineering: contractile behavior of musculoskeletal connective tissue cells. Tissue Eng. 2002;8(3):351-357.
36. Minuth WW, Strehl R, Schumacher K. Tissue Eng. – From Cell Biol. to Artificial Org. WILEY-VCH, Weinheim, 2005, 1.
37. Vunjak-Novakovic G. The fundamentals of tissue engineering: scaffolds and bioreactors. Novartis Found Symp. 2003;249:34-46.
38. Gardner RL. Stem cells and regenerative medicine: principles, prospects and problems. C R Biol. 2007 Jun-Jul;330(6-7):465-73.
39. Sohni A, Verfaillie CM. Mesenchymal stem cells migration homing and tracking. Stem Cells Int. 2013;2013:130763.
40. Moser B, Loetscher P. Lymphocyte traffic control by chemokines. Nature Immunology. 2001;2(2):123–128.
41. Peled A, Petit I, Kollet O, et al. Dependence of human stem cell engraftment and repopulation of NOD/SCID mice on CXCR4. Science. 1999;283(5403):845–848.

42. Müller A, Homey B, Soto H, et al. Involvement of chemokine receptors in breast cancer metastasis. Nature. 2001;410(6824):50–56.
43. Temenoff JS, Mikos AG. Review: tissue engineering for regeneration of articular cartilage. Biomaterials. 2000 Mar;21(5):431-40.
44. J.A. Buckwalter, H.J. Mankin. Articular cartilage: tissue design and chondrocyte–matrix interactions. AAOS Inst Course Lect, 47 (1998), pp. 477–486.
45. A.I. Caplan, B.D. Boyan. Endochondral bone formation: the lineage cascade. B.K. Hall (Ed.), Bone, CRC Press, Boca Raton, FL (1994), pp. 1–46.
46. Luminita Labusca, Udo Greiser, Viorel Nacu, Florin Zugun-Eloae and Kaveh Mashayekhi. Recent Patents on Regenerative Medicine 2014, 4, 52-68.
47. Bitton R. The economic burden of osteoarthritis. Am J Manag Care 2009;15(8 Suppl): 230-5.
48. Wang Y, Wei L, Zeng L, He D, Wei X. Nutrition and degeneration of articular cartilage. Knee Surg Sports Traumatol Arthrosc 2013; 21(8): 1751-62.
49. R.D. Coutts, R.L. Sah, D. Amiel. Effect of growth factors on cartilage repair. AAOS Inst Course Lect, 46 (1997), pp. 487–494.
50. J.A. Buckwalter. Articular cartilage: injuries and potential for healing. J Orthop Sports Phys Ther, 28 (1998), pp. 192–202.
51. Hunziker EB. Articular cartilage repair: are the intrinsic biological constraints undermining this process insuperable? Osteoarthritis Cartilage. 1999 Jan;7(1):15-28.
52. E.B. Hunziker, E. Kapfinger. Removal of proteoglycans from the surface of defects in articular cartilage transiently enhances coverage by repair cells. J Bone Jt Surg, 80-B (1998), pp. 144–150.

53. V.M. Goldberg, A.I. Caplan. Biologic resurfacing of articular surfaces. AAOS Inst Course Lect, 48 (1999), pp. 623–627.

54. S.D. Gillogly, M. Voight, T. Blackburn. Treatment of articular cartilage defects of the knee with autologous chondrocyte implantation. J Orthop Sports Phys Ther, 28 (1998), pp. 241–251.

55. F. Shapiro, S. Koide, M.J. Glimcher. Cell origin and differentiation in the repair of full-thickness defects of articular cartilage. J Bone Jt Surg, 75-A (1993), pp. 532–553.

56. S. Wakitani, T. Goto, R.G. Young, J.M. Mansour, V.M. Goldberg, A.I. Caplan. Repair of large full-thickness articular cartilage defects with allograft articular chondrocytes embedded in a collagen gel. Tissue Eng, 4 (1998), pp. 429–444.

57. J.E. Aston, G. Bentley. Repair of articular surfaces by allografts of articular and growth-plate cartilage. J Bone Jt Surg, 68-B (1986), pp. 29–35.

58. M. Brittberg, A. Lindahl, A. Nilsson, C. Ohlsson, O. Isaksson, L. Peterson. Treatment of deep cartilage defects in the knee with autologous chondrocyte transplantation. N Engl J Med, 331 (1994), pp. 889–895.

59. J.M. McPherson, R. Tubo, L. Barone. Letter to the editor. Arthroscopy, 13 (1997), pp. 541–543.

60. M. Brittberg, A. Lindahl, A. Nilsson, C. Ohlsson. Cellular aspects on treatment of cartilage injuries. Agents Actions Suppl, 39 (1993), pp. 237–241.

61. S. Shortkroff, L. Barone, H.P. Hsu, C. Wrenn, T. Gagne, T. Chi, H. Breinan, T. Minas, C.B. Sledge, R. Tubo, M. Spector. Healing of chondral and osteochondral defects in a canine model: the role of cultured chondrocytes in regeneration of articular cartilage. Biomaterials, 17 (1996), pp. 147–154.

62. R.C. Thomson, M.C. Wake, M.J. Yaszemski, A.G. Mikos. Biodegradable polymer scaffolds to regenerate organs. Adv Polym Sci, 122 (1995), pp. 245–274.
63. Kern S, Eichler H, Stoeve J, Kluter H, Bieback K. Comparative analysis of mesenchymal stem cells from bone marrow, umbilical cord blood, or adipose tissue. Stem Cells 2006; 24: 1294–301.
64. Zuk PA, Zhu M, Mizuno H et al. Multilineage cells from human adipose tissue: implications for cell-based therapies. Tissue Eng.2001; 7:211–28.
65. Gronthos S, Franklin DM, Leddy HA, Robey PG, Storms RW, Gimble JM. Surface protein characterization of human adipose tissue-derived stromal cells. J. Cell Physiol. 2001; 189: 54–63.
66. Zuk PA, Zhu M, Ashjian P et al. Human adipose tissue is a source of multipotent stem cells. Mol. Biol. Cell. 2002; 13: 4279–95.
67. Boone C, Mourot J, Gregoire F, Remacle C. The adipose conversion process: regulation by extracellular and intracellular factors. Reprod. Nutr. Dev. 2000; 40: 325–58.
68. Gimble JM, Guilak F. Differentiation potential of adipose derived adult stem (ADAS) cells. Curr. Top. Dev. Biol. 2003; 58: 137–60.
69. Zuk PA. Consensus statement. In: International Fat Applied Technology Society 2nd International Meeting. Pittsburg, PA, 2004.
70. Sekiya I, Larson BL, Smith JR, Pochampally R, Cui J-G, Prockop DJ. Expansion of human adult stem cells from bone marrow stroma: conditions that maximize the yields of early progenitors and evaluate their quality. Stem Cells 2002; 20: 530–41.
71. Mitchell JB, McIntosh K, Zvonic S et al. Immunophenotype of human adipose-derived cells:temporal changes in stromal-associated and stem cell-associated markers. Stem Cells 2006; 24: 376-85.

72. Sommer B, Sattler G. Current concepts of fat graft survival: histology of aspirated adipose tissue and review of the literature. Dermatol. Surg. 2000; 26: 1159–66.
73. Locke M, Windsor J, Dunbar PR. Human adipose-derived stem cells: isolation, characterization and applications in surgery. ANZ J Surg. 2009 Apr;79(4):235-44.
74. Bedini R, Ioppolo P, Pecci R, Filippini P, Caiazza S, Bianco A, Columbro G. Osservazioni di osso equino al microscopio elettronico a scansione e alla microtomografia 3D. Roma: Istituto Superiore di Sanità 2005 (Rapporti ISTISAN 05/37).
75. Laurencin C.T, Nair L.S. Nanotechnology and tissue engineering, the scaffold. CRC Press 2008.
76. B, Gerstenfeld LC, Einhorn TA, Spector M. Expression of smooth muscle actin in connective tissue cells participating in fracture healing in a murine model. Bone 2002; 30:738-745.
77. Kinner B, Spector M. Expression of smooth muscle actin in osteoblasts in human bone. J Orthop Res 2002; 20:622-632.
78. Martini F.H, Timmons M.J, Tallitsch R.B. Anatomia umana. Edises 2010; IV edizione.
79. Clarke B. Normal bone anatomy and physiology. Clin J Am Soc Nephrol 2008; 3:S131-9.
80. Burr DB. Targeted and nontargeted remodeling. Bone 2002; 30:2 –4.
81. Feng X, McDonald JM. Disorders of bone remodeling. Annu Rev Pathol 2011; 6:121-145.
82. Dimitriou R, Tsiridis E, Giannoudis PV; Current concept of molecular aspects of bone healing. Injury 2005; 36:1392-1404.
83. Fazzalari NL. Bone fracture and bone fracture repair. Osteoporosis international 2011; 22: 2003-6.

84. Pittenger M.F, Mackay A.M, Beck S.C, Jaiswal R.K, Douglas R, Mosca J.D, Moorman M.A, Simonetti D.W, Craig S, Marshak D.R. Multilineage potential of adult human mesenchymal stem cells. Science 1999; 284:143-7.
85. Einhorn T.A. The cell and molecular biology of fracture healing. Clin. Orthop. Relat. Res. 1998; S7-S21.
86. Granero-Molto F, Weis J.A, Miga M.I, Landis B, Myers T.J, O'Rear L, Longobardi L, Jansen E. D. Mortlock D.P, Spagnoli A. Regenerative effects of transplanted mesenchymal stem cells in fracture healing. Stem Cells 2009; 27:1887-1898.
87. Rose F.R.A.J, Oreffo R.O.C. Bone tissue engineering: hope vs hype. Biochemical and biophysical research communications 2002; 292:1-7.
88. Sittinger M, Bujia J, Rotter N, Reitzel D, Minuth WW. and Burnmester GR. Tissue engineering and autologous transplant formation: practical approaches with resorbable biomaterials and new cell culture techniques. Biomaterials 1996; 17: 237-242.
89. Ikada Y. Challenges in tissue engineering. J.R. Soc. Interface 2006; 3:589-601.
90. Alsberg E., Kong HJ, Hirano Y, Smith MK, Albeiruti A, Mooney D.J. Regulating bone formation via controlled scaffold degradation. J Dent Res 2003; 82:903-908.
91. Lu W, Ji K, Kirkham J, Yan Y, Boccacini AR, Kellet M, Jin Y, Yang X.B. Bone tissue engineering by using a combination of polymer/Bioglass composites with human adipose-derived stem cells. Cell Tissue Res 2014: 10.1007 .
92. Nobes, C. and Hall A. Regulation and function of the Rho subfamily of small GTPases. (1994) Curr. Opin. Genet. Dev. 1994; 4:77–81.
93. Zhang J, King W.G, Dillon S, Hall A, Feig L, Rittenhouse S.E. Activation of platelet phosphatidylinositide 3-kinase requires the small GTP-binding protein Rho. J Biol Chem. 1993; 268:22251-54.

94. Chong LD, Traynor-Kaplan A, Bokoch GM, Schwartz MA. The small GTP-binding protein Rho regulates a phosphatydilinositol 4-phosphate 5-kinase in mammalian cells. Cell 1994; 79:507-513.
95. Hill CS, Wynne J, Treisman R. The Rho family GTPases RhoA, Racl, and CDC42H regulate transcriptional activation by SRF. Cell 1995; 81:1159-1170
96. Amano M, Ito M, Kimura M, Fukata Y, Chihara K, Nakano T, Matsuura Y, Kaibuchi K. Phosphorylation and activation of Myosin by Rho-associated kinase (Rho-kinase). J.Biol.Chem 1996; 271: 20246-49.
97. Nobes CD, Hall. Rho, rac and cdc42 GTPases regulate the assemby of multi molecular focal complexes associated with actin stress fibers, lamellipodia and filopodia. Cell 1995; 81:53-62.
98. Etienne-Manneville S, Hall A. Rho GTPases in cell biology. Nature 2002; 420(6916): 629–35.
99. Tapon N, Hall A. Rho, rac and cdc42 GTPase regulate the organization of the actin cytoskeleton. Curr Opin Cell Biol 1997; 9:86-92.
100. Maekawa M et Al. Signaling from Rho to the actin cytoskeleton through protein kinases ROCK and LIM-kinase. Science 1999; 285: 895-8.
101. Burridge K, Chrzanowska WM. Focal adhesions, contractility, and signaling. Ann Rev Cell Dev Biol 1996; 12:463-518.
102. Riento K, Ridley AJ. Rocks: multifunctional kinases in cell behaviours. Nat Rev Mol Cell Biol 2003; 4 (6): 446–56.

103. Kamioka H., SugawaraY., Honjo T., Yamashiro T., Takano- Yamamoto T. Terminal differentiation of osteoblast to osteocytes is accompanied by dramatic changes in the distribution of actin-binding proteins. J. Bone Miner Res 2004; 19: 471-8.

104. Tamariz E., Grinnell F. Modulation of fibroblast morphology and adhesion during collagen matrix remodeling. Mol. Biol. Cell 2002; 13: 3915-3929.

105. Tigyi, G. Physiological responses to lysophosphatidic acid and related glycero-phospholipids. Prostaglandins 2001; 64: 47–62.

106. Umezu-Goto M., Kishi Y., Taira A., Hama K., Dohmae N., Takio K., et al. Autotaxin has lysophospholipase D activity leading to tumor cell growth and motility by lysophosphatidic acid production. J Cell Biol 2002; 158: 227-33.

107. Takamitsu Sano, Daniel Baker, Tamas Virag, Atsushi Wada, Yutaka Yatomi, Tetsuyuki Kobayashi, Yasuyuki Igarashi and Gabor Tigyi. Multiple Mechanisms Linked to Platelet Activation Result in Lysophosphatidic Acid and Sphingosine 1-Phosphate Generation in Blood. J. Biol. Chem. 2002; 277:21197-21206.

108. Panupinthu N, Rogers JT, Zhao L, Solano-Flores LP, Possmayer F, Sims SM, Dixon SJ. P2X7 receptors on osteoblast couple to production of lysophosphatidic acid: a signaling axis promoting osteogenesis. J Cell Biol. 2008; 181: 859-71.

109. Choi JW, Herr DR, Noguchi K, Yung YC, Lee CW, Mutoh T, Lin ME, Teo ST, Park KE, Mosley AN, Chun J. LPA receptors: subtypes and biological actions. Annu Rev Pharmacol Toxicol 2010; 50: 157-86.

110. Lee H, Goetzl EJ, An S. Lysophosphatidic acid and sphingosine 1-phosphate stimulate endothelial cell wound healing. Am J Physiol Cell Physiol. 2000; 278:C612-8.

111. Themistocleous GS, Kontou SE, Lembessis P, Katopodis HA, Kaseta MA, Themistocleous MS. Skeletal growth factor involvement in the regulation of fracture healing process. *In vivo* 2003; 17:489-503.

112. Dziak R, Yang BM, Leung BW, Li S, Marzec N, Margarone J, Bobek L. Effects of sphingosine-1-phosphate and lysophosphatidic acid on human osteoblastic cells. Prostaglandins 2003; 68:239-249.

113. Lee C.W, Rivera R, Dubin A.E, Chun J. LPA(4)/GPR23 is a lysophosphatidic acid (LPA) receptor utilizing G(s)-, G(q)/G(i)-mediated calcium signaling and G(12/13)-mediated Rho activation. J Biol Chem. 2007; 282:4310-7.

114. Karagiosis S. A, Chrisler W. B, Bollinger N, Karin N. J. Lysophosphatidic acid-induced ERK activation and chemotaxis in MC3T3-E1 preosteoblasts are independent of EGF receptor transactivation. J. Cell. Physiol. 2009; 219:716-723.

115. Mansiello LM, Fotos JS, Galileo DS, Karin NJ. Lysophosphatidic acid induces chemotaxis in MC3T3-E1 osteoblastic cells. Bone 2006; 39:72-82.

116. Gidley J, Openshaw S, Pring ET, Sale S, Mansell JP. Lysophosphatidic acid cooperates with 1α,25(OH)2D3 in stimulating human MG63 osteoblast maturation. Prostaglandins Other Lipid Mediat. 2006; 80:46-61.

117. Liu Y.B, Kharode Y, Bodine P.V.N, Yaworsky P.J, Robinson J.A, Billiard J. LPA Induces Osteoblast Differentiation Through Interplay of Two Receptors: LPA1 and LPA4. Journal of Cellular Biochemistry 2010; 109:794-800.

118. Mansell J.P, Barbour M, Moore C, Nowghani M, Pabbruwe M, Sjostrom T, Blom A.W. The synergistic effects of lysophosphatidic acid receptor agonist and calcitriol on MG63

osteoblast maturation at titanium and hydroxyapatite surfaces. Biomaterials 2010; 31:199-206.

119. Mansell J.P, Nowghani M, Pabbruwe M, Paterson I.C, Smith A.J, Blom A.W. Lysophosphatidic acid and calcitriol co-operate to promote human osteoblastogenesis: requirement of albumin-bound LPA. Prostaglandins and Other Lipid Mediators 2011, 95:45-52.

120. Grinnel F, Ho C, Tamariz E, Lee DJ, Skuta G. Dendritic fibroblast in three-dimensional collagen matrices. Mol Biol Cell 2003; 14:384-95.

121. Hadidi P, Athanasiou KA. Enhancing the mechanical properties of engineered tissue trough matrix remodeling via the signaling phospholipid lysophosphatidic acid. Biochem Biophys Res Commun 2013; 29:133-8.

122. Elsdale T and Bard J. Collagen substrata for studies on cell behavior. The Journal of Cell Biology 1972; 54:626-637.

123. Reinert H, Jundt G. In situ measurement of collagen synthesis by human bone cells with a Sirius Red-based colorimetric microassay: effects of TGFβ2 and ascorbic acid. Histochem Cell Biol. 1999; 112:271-276.

124. Bosetti M, Boccafoschi F, Leigheb M, Cannas M. Effect of different growth factors on human osteoblasts activities: a possible application in bone regeneration for tissue engineering. Biomolecular Engineering 2007; 24:613-618.

125. Parreno J, Buckley-Herd G, de-Hemptinne I, Hart DA. Osteoblastic MG-63 cell differentiation, contraction, and mRNA expression in stress-relaxed 3D collagen I gels. Mol Cell Biochem (2008) 317:21-32.

126. Suarez-Gonzalez D, Lee JS, Diggs A, Lu Y, Nemke B, Markel M, Hollister SJ, Murphy WL. Controlled multiple growth factor delivery from bone tissue engineering scaffolds via designed affinity. Tissue Eng Part A 2014; 20:2077-2087.

127. Grey A, Chen Q, Callon K, Xu X, Reid IR, Cornish. The phospholipids sphingosine-1-phosphate and lysophosphatidic acid prevent apoptosis in osteoblastic cells via a signalling pathway involving G(i) proteins and phosphatidylinositol-3 kinase. Endocrinology 2002; 143:4755-63.

128. Sims SM, Panupinthu N, Lapierre DM, Pereverzev A, Dixon SJ. Lisophosphatidic acid: a potential mediator of osteoblast-osteoclast signalling. Biochimica et Biophysica Acta (2013) 1831:109-116.

129. Bosetti M, Fusaro L, Nicolì E, Borrone A, Aprile S, Cannas M. Poly-L-lactide acid modified scaffolds for osteoinduction and osteoconduction. J Biomed Mater Res Part A 2014; 102A:3531-3539.

130. Kimura, K., Ito, M., Amano, M., Chihara, K., Fukata, Y., Naka- fuku, M., et al. Regulation of myosin phosphatase by Rho and Rho-associated kinase (Rho-kinase). Science 1996; 273(5272): 245–248.

131. Parizi M, Howard E.W, Tomasek J. Regulation of LPA-Promoted Myofibroblast Contraction: Role of Rho, Myosin Light Chain Kinase, and Myosin Light Chain Phosphatase. Experimental Cell Research 2000; 254: 210-220.

132. Lee, D.J., Ho, C.H., and Grinnell, F. LPA-stimulated fibroblast contraction of floating collagen matrices does not require Rho kinase activity or retraction of fibroblast extensions. Exp. Cell Res. 2003; 289(1): 86–94.

6. List of Publications

- **Papers**

1) Bosetti M, Borrone A, Follenzi A, Messaggio F, Tremolada C, Cannas M. Human lipoaspirate as autologous injectable active scaffold for one-step repair of cartilage defects. Cell Transplant. 2015 Sep 21. [Epub ahead of print] PubMed PMID: 26395761.

2) Sabbatini M, Moalem L, Bosetti M, Borrone A, Boldorini R, Taveggia A, Verna G, Cannas M. Effects of erythropoietin on adipose tissue: a possible strategy in refilling. Plast Reconstr Surg Glob Open. 2015 Apr 7;3(3):e338. PubMed PMID: 26034645.

3) Bosetti M, Sabbatini M, Calarco A, Borrone A, Peluso G, Cannas M. Effect of retinoic acid and vitamin D3 on osteoblast differentiation and activity in aging. J Bone Miner Metab. 2016 Jan;34(1):65-78. PubMed PMID: 25691285.

4) Bosetti M, Fusaro L, Nicolì E, Borrone A, Aprile S, Cannas M. Poly-L-lactide acid-modified scaffolds for osteoinduction and osteoconduction. J Biomed Mater Res A. 2014 Oct;102(10):3531-9. PubMed PMID: 24178410.

- **Abstracts**

5) Leigheb M, Bosetti M, Borrone A, Marcuzzi A, Cannas M (2015). Purpose Of A Novel Bioactive Composite Device For Ligament Regenerative Substitution. THE JOURNAL OF HAND SURGERY, 40E(S1):129-130.

6) Bosetti M, Fusaro L, Borrone A, Nicolì E, Cannas M (2014). Injectable Bone-Graft Substitute For *In Vivo* Tissue Regeneration. Italian Journal Of Anatomy And Embriology 118(2):33 (2013). 67° Italian Society Of Anatomy And Histology, 20-22 Settembre, Brescia.

7) Bosetti M, Borrone A, Colli C, Ventura C, Cannas M (2014). Can Human Lipoaspirate Be Considered An Autologous Injectable Scaffold To Repair Cartilage Defects? Cellr-4repair, Replacement, Regeneration & Reprogramming.

7. Acknowledgements

I would like to thank my PhD coordinator Prof.ssa Marisa Gariglio and my PhD tutor Prof. Mario Cannas. I also would like to thank Prof.ssa Michela Bosetti. I am grateful for the trust they placed in me to undertake this project and for their competence in guiding my work.

Special thanks also go to all the laboratory of Human Anatomy with whom I have shared great experiences and interesting discussions.

Finally, I would like to thank Prof.ssa Antonia Follenzi from the Histilogy Lab, Dr. Massimiliano Leigheb from the Major Hospital of Novara, Dr. Carlo Tremolada from IMAGE Institute (Milan), Dr.ssa Fanuel Messaggio from Diabetes Research Institute (University of Miami, Florida, USA), Dr. Pierre Layrolle and Dr.ssa Stefania Pianta from Faculté de Médecine INSERM UMR 957_LPRO (Nantes, France) for their collaboration.